UNCLASSIFIED

AD **405 909**

DEFENSE DOCUMENTATION CENTER

FOR

SCIENTIFIC AND TECHNICAL INFORMATION

CAMERON STATION, ALEXANDRIA, VIRGINIA

UNCLASSIFIED

Studies of Primary Electron Sources

W. G. SHEPHERD, Chief Investigator
Report Prepared by D. E. ANDERSON

ELECTRON TUBE RESEARCH LABORATORY
UNIVERSITY OF MINNESOTA
INSTITUTE OF TECHNOLOGY

Scientific Report No. 5
March 1, 1962 to June 1, 1962
January 1963

Prepared for

ELECTRONICS RESEARCH DIRECTORATE
AIR FORCE CAMBRIDGE RESEARCH LABORATORIES
OFFICE OF AEROSPACE RESEARCH
UNITED STATES AIR FORCE
BEDFORD, MASSACHUSETTS

DDC

JUN 10 1963

TISIA D

Requests for additional copies by Agencies of the
Department of Defense, their contractors, and other
Government agencies should be directed to the:

ARMED SERVICES TECHNICAL INFORMATION AGENCY
ARLINGTON HALL STATION
ARLINGTON 12, VIRGINIA

Department of Defense contractors must be established
for ASTIA services or have their "need-to-know" certified
by the cognizant military agency of their project or
contract.

All other persons and organizations should apply to
the:

U. S. DEPARTMENT OF COMMERCE
OFFICE OF TECHNICAL SERVICES
WASHINGTON 25, D. C.

Table of Contents

I.   Abstract

A new chemical activation tube using carbon as an acti-
vator has been constructed, and preliminary results indicate
that the basic design is satisfactory.

A theoretical analysis of the thermal changes occurring
in an oxide cathode during long pulse current drain is presented.
The set of nonlinear equations resulting from the analysis is
solved numerically through the use of a digital computer, and
the solutions obtained are discussed in terms of the experimen-
tal results.   In particular, the solution indicates that a
thermal instability can occur, and predicts the dependence of
this "sparking threshold" on cathode activity and current
density.

A series of experiments aimed at investigating the in-
fluence of the coating thickness on cathode parameters was
continued.   A tube was constructed and processed, but because
of coating cracking and difficulty encountered in temperature
measurements, insufficient data for quantitative analysis of
the thickness dependence were obtained.   The preliminary re-
sults suggest that the thicker coatings give rise to higher
pulsed emission levels.

Photoemission studies of BaO on a passive base illustrate
the role of chemical activation and electrolytic activation of
the coating.   Thermionic and photoemission data obtained from
a thin film BaO coating on an active base are presented and
the effect of the environment of the coating investigated.   The

effect of glass charging on the total photoelectric yield and on the determination of the zero of energy in the energy distribution structure is described and methods for eliminating the effect are discussed.

Two attempted methods of forming thin continuous oxide films on vacuum-deposited Al and Be layers by reaction with an oxygen atmosphere are discussed.

A system for monitoring the complex impedance of tunnel current devices is described and preliminary results are presented, for an Al-Al$_2$O$_3$-Al sample, in the form of an equivalent parallel RC network, where R and C are both functions of time and of the dc bias voltage.

Techniques have been developed to allow preparation of metallic and insulating films by sputtering in an inert-gas discharge. These techniques have been applied to produce films of MgO which were insulating, although evidently not continuous. The sputtering technique has also been applied to produce Ta films suitable for use as substrate materials for Ta-Ta$_2$O$_5$-M samples. The results obtained with the sputter-deposited Ta samples are similar to those obtained with Ta samples prepared by other methods.

II. Studies of Thermionic Cathodes

1. Introduction

The studies to be reported in this section are all directed to obtaining an understanding of the alkaline-earth metal oxides as thermionic cathodes. While other systems will be investigated later, it is felt that the present understanding of the oxide cathode is such as to make specific studies of this system most fruitful at the start.

The purpose of this introduction then is to review the groundwork on which these researches are based, to summarize briefly the important results of our previous work,* and to present the general outline of the plan by which the particular objectives of the research are being approached. We hope that such a resume will serve to relate the individual experiments to the program as a whole.

There is general agreement that the oxide cathode is an n-type semiconductor and that an excess of alkaline-earth metal in the coating is essential for high emission. It is not necessary to assume that this excess metal must occur in the grains of the coating in order to provide donors, but only that the presence of free metal in the pores is necessary for the production of donors. This excess metal is believed to result largely from the action of reducing impurities incorporated in the base nickel. It might reasonably be expected that the evaporation

rate of free alkaline-earth metal from the oxide coating would serve as an indication of the rate at which this free metal is being produced by chemical reduction. Thus, the evaporation rates of such free metal might be correlated with the emission capabilities of the cathode.

As a convenient and accurate means for measuring the rate at which the alkaline-earth metal is evolved from the coating, radioactive tracers of Ba or Sr can be incorporated in the oxide coating. This method allows one to monitor the total amount of alkaline-earth metal being evolved from the coating, either as the oxide or as the free metal. Although the total amount of Ba evaporated (Ba and BaO) is larger than that of Sr (Sr and SrO), our observation is that the metal-to-oxide ratio is more favorable for the detection of Sr metal than for Ba metal in the presence of the background of oxide evaporation.

Subsequent experiments were designed to determine whether a correlation existed between the Sr evaporation and the emission from oxide-coated cathodes. For these experiments cathodes based on single additive nickel alloys and on pure nickel doped with carbon have been used. A correlation between Sr evaporation and the development of emission has been observed for both types of cathode base. This correlation has been qualitatively explained using a model in which the strontium evolution follows the rate at which the reducing agent arrives by diffusion at the base nickel-oxide interface. The emission is taken as being controlled by the donor concentration in the oxide particles,

with the generation of additional donors at the surface of each particle being a function of the pressure of free alkaline-earth metal in the pores of the coating.

It has been found that, for the concentrations studied, single additive alloys of Al, Mn, W, Mg, and Si in Ni lead to a rate of coating reduction which is limited by the diffusion of the reducing element to the oxide coating-base metal interface. In these cases the rate of reduction is proportional to $t^{-1/2}$ where t is the total operating time. Quantitative agreement with observed data can be obtained when the diffusion coefficient of each additive in nickel is known; these values have been determined. Early studies of the pulse emission from cathodes based on these alloys indicated that, following an initial activation, the emission declined monotonically with cathode life. It is postulated that this decline is a consequence of competing processes and that, under ideal conditions, stable emission levels should be maintained even for the systems with declining rates of chemical reduction. This "stable donor" behavior has been observed with cathodes based on Mg-Ni and Al-Ni alloys.

It is possible to devise a cathode base from which carbon can be dispensed to the coating at a rate which is constant over extended periods of time. The Sr evolution from coatings based on such a dispenser is found to be constant. This system is of considerable interest because of the possibility of producing chemical reduction of the coating at a constant and controllable rate.

All of the foregoing studies have been made with the cathode in thermal equilibrium at a fixed temperature. A complete understanding of the factors affecting chemical activation demands information as to their temperature dependence. An experimental investigation of the response of oxide cathodes to step changes in temperature has been made which shows both short-term and long-term changes, corresponding respectively to (1) the fraction of the donors thermally ionized and (2) changes in the equilibrium concentration of donors.

Anode poisoning of an oxide cathode, caused by drawing current to an electrode which has accumulated evaporation products from the cathode, has been studied with respect to the change in activity during such poisoning and to subsequent recovery. The pulse emission under these conditions may drop from $amps/cm^2$ to $milliamps/cm^2$ with an apparent exponential decay having a time constant of a few minutes. It is known from other studies made in these laboratories that there is a low-voltage threshold for the dissociation of anode deposits or desorption of gas layers. If the anode bombardment is stopped when the emission has fallen to a stable level, the pulse emission then recovers in a manner very closely resembling the initial chemical activation of the cathode. It has been shown that the material which dissociates under electron bombardment is an impurity, rather than the oxides, related to the bakeout of the envelope of the structure.

Two major processes can contribute to the activation of the oxide cathode. These are chemical activation due to reducing agents incorporated in the base metal and electrolytic activation of the coating. The effect of chemical activation has been studied by operating the cathodes without current drain during life. Early attempts to produce simple electrolytic activation by drawing a continuous current from an oxide cathode based on a passive nickel led to activity levels which were much lower than could be achieved from cathodes based on active nickels in which chemical activation played a role. The results of studies of bombardment-induced poisoning suggested that this competing process limited the development of electrolytic activation. Accordingly, a structure was developed which permits the drawing of a continuous current to a positive grid located so close to the cathode that the threshold for anode poisoning would not be exceeded. Under these conditions, a very pronounced activation of the cathode occurred when continuous current was drawn through the coating. It was found that the cathode activated with a time constant of the order of 10 minutes at 1119°K, and also that a continuation of current drain for several hours resulted in the development of a stable level of activity which then persisted even when current drain was discontinued.

These results have been interpreted in terms of a model in which the donors are not volatile and are thus stable in the absence of competing processes. A continuous current drain

leads to a field-enhanced preferential evolution of anions from the coating with a corresponding increase in donor concentration, and emission capability, at the surface of the individual oxide grains. The permanent activation is viewed as the result of a saturation of the bulk of the oxide particles by the presence of this excess donor concentration at the surface.

The apparent emission measured from an oxide cathode by a method dependent on the deviation from a three-halves power law is influenced by the resistive drop in the oxide coating. This drop can develop across a resistance appearing at the interface between the oxide coating and the base metal and also across a resistance occurring in the bulk oxide. Studies of the formation of resistive interface layers for various reducing impurities have shown that only in the case of silicon is a significant resistive interface layer developed. The bulk resistive effects can be compensated by suitable measuring instrumentation and thereby an accurate determination of the saturation pulse emission and of the coating resistance can be made. The necessary instrumentation to permit this has been developed in this laboratory. The deviation of a plot of (i) vs. $(v-ki)$ is observed with k adjusted to fit a 3/2 power space-charge curve. As a measure of the saturation emission, either J_{20} (the current at which the I-V trace has fallen 20% below the space-charge law) or J_d (the current at which deviation begins) can be determined.

2. Controlled Activation and Deactivation of Oxide

Cathodes
R. H. Springer

During this interval work has been continued on controlled chemical activation studies using carbon as an activator. The major goal of the present study is to examine the effects of oxygen on an oxide-coated cathode held in a constant state of activity by a reduction of the coating with carbon. It is desired to have a system whereby the reduction rate of a single cathode can be varied, thus reducing the scatter which is introduced from physical and environmental changes from tube to tube.

A new tube structure, which incorporates several features of tubes used earlier in this study,* has been designed. This tube, KT1BB, is shown in Fig. 1. The essential feature of this structure is a Kovar partition, 0.005" thick, which is heli-arc welded over the end of a Varian vacuum flange. The Kovar partition, which has 0.010" thick 0.125" diameter pure Ni disks welded to the center of each side, divides the tube into two separate sections, labeled experimental and bombardment in the figure. Both sections are continuously pumped by separate Ti sputter pumps throughout the life of the tube.

As shown in the detail of Fig. 1, the Ni disk in the experimental section of the tube serves as the base for the oxide-coated cathode under study. The cathode contains a radioactive

*Studies on Base Nickels for Oxide-Coated Cathodes, Contract No. AF 19(604)-3890, Final Report, p. 39.

Sr^{89} tracer to measure the evolution products during life. The pulsed emission and Sr evolution are measured with separate Ti anodes designed to be moved into place in front of the cathode on a tungsten trolley by an external magnet. The anodes are counted through a 0.0015" Kovar window placed in one sidearm of the tube.

The Ni disk in the bombardment section has four tabs welded around the edge for carbon application during life. The cathode is heated by electron bombardment from a tungsten filament and the temperature is measured by a Pt/Pt + Rh thermocouple, which is not shown in the figure, welded to the disk in the bombardment section.

In operation the cathode is held at constant temperature. When equilibrium levels of pulse emission and Sr evolution have been attained, the flange is then opened and carbon encapsulated in Ni is welded to the tabs. The base is thus changed from passive to active without disturbing the equilibrium in the experimental section of the tube.

Passive-based conditions can be restored by cutting off the source and allowing the remaining carbon to diffuse to the coating. This operation can be cycled three or four times on a given cathode before depletion effects become prominent. The rate of carbon arrival at the coating is inversely proportional to the diffusion path length so that succeeding cycles provide higher reduction rates.

This tube was preprocessed and left evacuated until immediately before coating the cathode disk with $(BaSr)CO_3$ which contained radioactive Sr^{89} as a tracer. The tube was then sealed to the pump station and processed following the standard schedule presented in a previous report.*

The tube was sealed off and the associated sputter pumps put in operation. The cathode was operated until at 400 hours life the pulse emission had reached a stable level of $0.5\,amps/cm^2$. At this time the envelope developed a leak, terminating the experiment on this tube. A new tube is being constructed with modifications in the bombardment system and thermocouple arrangement, which were indicated by the operation of KT1BB to make the tube more reliable.

3. Long Pulse Performance of Oxide-Coated Cathodes

D. A. Campbell

In the previous report of this series an emission enhancement was described which occurred during long pulse current drain to a "clean" anode. It was found that the details of the experimentally observed phenomena were consistent with a model which describes temperature changes that occur in the oxide coating during long pulse current drain. The model involved a linearized solution to the heat equation which was valid for small temperature changes.

*Studies on Base Nickels for Oxide-Coated Cathodes, Contract No. AF 19(604)-3890, Scientific Report No. 2.

To describe large temperature changes which occur in the oxide coating when sufficient voltage is applied to a diode so that the emission is saturated over the entire range of temperature change, we must solve

$$\frac{\partial T}{\partial t} = K \frac{\partial^2 T}{\partial x^2} + \frac{J_s^2 \rho}{c\delta} , \tag{1}$$

subject to the boundary conditions,

$$T(0,t) = T_0 \tag{2}$$

$$T(x,0) = T_0 - \frac{\beta T^4(L,0)x}{k} \tag{3}$$

$$- k \left. \frac{\partial T}{\partial x} \right|_{x=L} = J_s \chi + \beta T^4(L,t) \tag{4}$$

where $T = T(x,t)$ is the temperature, t is the time variable, x is the spatial variable, k is the thermal conductivity, $K = \frac{k}{c\delta}$ is the thermal diffusivity, c is the heat capacity, δ is the density, $\rho = \frac{1}{\sigma}$ is the resistivity, J_s is the current density and β is a constant proportional to emissivity of the oxide. Both J_s and σ are temperature dependent.

The temperature dependence of J_s is assumed to be given by the saturation emission, J_0, predicted by the Fowler emission equation

$$J_s = J_0 = n_d^{1/2} AT^{5/2}(L,t) \exp\left[-e(\chi + \frac{1}{2}\varepsilon_d)/k_B T(L,t) \right] \tag{5}$$

and the temperature dependence of the conductivity is given by

$$\sigma = n_d^{1/2} \, S T^{1/4}(x,t) \, \exp\left[- e\varepsilon_d/2kT(x,t)\right] \qquad (6)$$

where n_d = donor density

$A = 2ek_B(2\pi m^*k_B)^{1/4}/h^{3/2}$

χ = electron affinity

ε_d = energy difference between the donor level and the bottom of the conduction band

$S = \dfrac{4\sqrt{2}\,e^2 \ell_0}{3\,h^{3/2}} (2\pi m^*k_B)^{1/4}$

ℓ_0 = mean free path of an electron

m^* = effective mass of an electron

k_B = Boltzmann's constant

h = Planck's constant

T = absolute temperature

e = electronic charge.

The assumption that J_s is given by the zero-field value neglects the Schottky effect. If the Schottky effect were considered the saturated current would be given by
$J_s = J_0 \exp(+ b e \sqrt{eE}/k_B T)$ where b is a constant, and E is the electric field at the coating surface. It can be shown that the "Schottky correction" changes by less than an order of magnitude for a twofold change in temperature whereas J_0 changes by a factor of 3×10^3 assuming $(\chi + \frac{1}{2}\varepsilon_b) = 1.4$ eV. Since the temperature dependence of J_0 is much stronger than that of the "Schottky factor", temperature increases calculated assuming

$J_s = J_o$ will give values representing a lower bound which will be quite close to the actual temperature increase. Further, the assumed condition ($J_s = J_o$) will become a progressively better assumption as temperature increase occurs during a pulse.

Substituting Eqs. (5) and (6) into Eqs. (1) - (4) gives

$$\frac{\partial T(x,t)}{\partial t} = K \frac{\partial^2 T(x,t)}{\partial x^2} + \frac{n_d^{1/2} A^2 T^{5/2}(L,t) \exp\left[-2\,\Phi/T(L,t)\right]}{S T^{1/4}(x,t) \exp\left[-\Theta/T(x,t)\right]} \quad (7)$$

subject to

$$T(0,t) = T_o \quad (8)$$

$$T(x,0) = T_o - H(0)\, x/k \quad (9)$$

$$- k \left. \frac{\partial T(x,t)}{\partial x}\right|_{x=L} = n_d^{1/2} \chi A T^{5/4}(L,t) \exp\left[-\Phi/T(L,t)\right] + \beta T^4(L,t) \quad (10)$$

where

$$\Phi = e(\chi + \tfrac{1}{2}\varepsilon_d)/k_B$$

$$\Theta = \varepsilon_d/2k_B$$

$H(0)$ = the power loss by radiation at $x = L$ and $t = 0$

β = a constant proportional to the emissivity of the oxide.

This nonlinear set of equations cannot be solved analytically, but a numerical solution can be obtained. For a numerical solution

the boundary value problem must be formulated as a set of difference equations. We divide the coating from $x = 0$ to $x = L$ into $(N - 1)$ intervals of width $\Delta x = L/(N - 1)$. A convenient scale factor for the time increment, Δt, is defined by $\Delta t = (\Delta x)^2/2K$. Considering a point in the x, t plane specified by the indices i, j gives

$$T(i, j+1) = \frac{1}{2}\left[T(i + 1, j) + T(i - 1, j)\right] +$$

$$\frac{(\Delta t)n_d^{1/2}A^2T^{5/2}(N,j)\exp\left[- 2\phi/T(N,j)\right]}{ST^{1/4}(i,j)\exp\left[-\phi/T(i,j)\right]} \tag{11}$$

subject to

$$T(1,j) = T_0 \tag{12}$$

$$T(i,1) = T_0 - H(0)iL/(N - 1)k \tag{13}$$

$$T(N,j) - T(N - 1,j) = - \frac{L}{k(N - 1)}\left[n_d^{1/2}A\chi T^{5/4}(N,j)\exp\left[-\phi/T(N,j)\right]\right.$$

$$\left. + \beta T^4(N,j)\right] \tag{14}$$

where Eqs. (11) - (14) are the difference equations which correspond to the differential Eqs. (1) - (4).

Numerical solutions to the set of difference equations have been obtained using a digital computer to carry out the

calculations.* An outline of the program is given in Appendix 2.
The parameters T_o and n_d were allowed to take on a range of
values which were considered typical for oxide cathodes. The
constants, A in the emission equation, Eq. (5), and S in the
expression for the conductivity, Eq. (6), were chosen to bring
the calculated values of the emission and conductivity into
agreement with those observed experimentally, assuming a value
of 10^{18} cm^{-3} for n_d.

The calculations give the temperature on a lattice of
points in the x,t plane. This is demonstrated in Fig. 2 where
the calculated values of temperature are plotted as a function
of position with time as a parameter for typical values of n_d
and T_o. It is noted that the temperature at positions internal
to the oxide tend to be uniform. This indicates that heat
generated in the interior of the oxide does not diffuse to the
surfaces, which is to be expected since the thermal time con-
stant for the oxide is large with respect to the time durations
being considered.

Only a small fraction of the points involved in the com-
puter calculation were read out. Accordingly the end points
have been connected to the first interior point by dotted lines,
since one might expect that the essentially uniform temperature
values of the interior will extend close to the surface. This
conjecture is based on a calculation of the thermal diffusion

*A Fortran program was developed for the CDC Type 1604
digital computer.

length, which yields a value of about one-tenth the coating thickness for 100 μsec pulse durations.

In Fig. 3 the maximum temperature in the oxide layer, T_{max}, is plotted as a function of time after the initiation of saturation current drain, for the data of Fig. 2. It is observed that a gradual temperature rise is followed by a very rapid increase. Arbitrarily we have taken as a critical time, t_c, the time required for T_{max} to reach 2000°K which is near the melting point of the alkaline-earth oxides. Log-log plots of t_c vs. donor density are shown in Fig. 4 for three values of T_o. The slope of these curves is nearly $(-\frac{1}{2})$, implying that $t_c n_d^{1/2}$ (and hence $t_c J_{so}$, where J_{so} is the value of J_s at $t = 0$) is essentially constant.

It is interesting to note that this result is in accord with the theory (see Appendix 1) for a simplified model is which the thermal losses by radiation, emission cooling, and heat conduction are neglected. The initial emission level J_{so} as a function of n_d is shown in Fig. 5. Semilog plots of t_c vs. $10^4/T_o$ are shown in Fig. 6. It is observed that the slope of these curves are approximately equal to $2\phi - \theta$. This is also in accord with the theory of the simplified model.

There are two reasons why the simplified model is in accord with the more general solution, (1) the thermal diffusivity for the oxide is sufficiently small so that the heat generated in the interior of the oxide layer cannot diffuse to the surface during the time intervals of interest, and (2) the

temperature dependence of the Joule heating, $J^2\rho$, is much stronger than the temperature dependence of the emission cooling, $J\chi$, and the surface radiation, βT^4.

The thermal instability predicted by our model is similar to the phenomenon O'Dwyer in his review paper "Dielectric Breakdown in Solids" has called Impulse Thermal Breakdown.* The distinguishing feature of the runaway process considered here is the very strong temperature dependence of the thermal driving force, $(J^2\rho)$. This comes about of course because of the strong temperature dependence of thermionic emission. As a consequence of this runaway feature of the Joule heating, a catastrophic event occurs in time intervals much shorter than those usually associated with thermal breakdown in insulators.

The numerical solution as well as the simplified model has predicted that the product of the critical time, t_c, and the initial current density, J_o, is a constant. A connection between the thermal instability and cathode sparking is implied by the fact that a similar relationship between the pulse duration, t_p, and the pulse current at the "sparking threshold", J_{sp}, is observed experimentally in oxide cathodes (i.e., $t_p J_{sp} = \text{constant}$).**

* J. J. O'Dwyer, Phil. Mag. Suppl. <u>7</u>, No. 27, 349 (July 1958).

**R. M. Matheson and L. S. Nergaard, J. Appl. Phys. <u>23</u>, 869 (1952).
   L. S. Nergaard, RCA Review <u>13</u>, 477 (1952).

From the expression for t_c given in Appendix 1 we can write

$$t_c \approx \frac{c\, \delta\, T_o^2}{J_o^2\, \rho_o}$$

where J_o and ρ_o are the saturated current and the resistivity at $t = 0$ or $T = T_o$. For a pulse of fixed duration the above equation predicts a catastrophic event (thermal breakdown) at constant values of $J_o^2 \rho_o$. The observation of Eisenstein* that, for 1 μsec pulses, cathode sparking occurs at constant values of $I^2 R$ (I = sparking current, R = coating resistance) provides further support of our hypothesis that cathode sparking is related to thermal instability.

A rough calculation of the diffusion length for 100 μsec periods gives a value (6 x 10^{-4} cm) which is small with respect to the lateral dimension of the cathode. This fact indicates that localized hot spots could easily occur in the nonuniform situation which prevails in a practical oxide emitter. The phenomenon of space charge limited sparking, described by Coomes,** could be explained on this basis if a high current density were to develop in a localized patch. The high current density could result, for example, as a consequence of a localized space-charge neutralization, resulting from transient generation of positive ions.

* A. S. Eisenstein, J. Appl. Phys. 20, 776 (1949).
**E. A. Coomes, J. Appl. Phys. 17, 647 (1946).

The calculation of thermal diffusion lengths for various diffusion times provides an estimate of the range of coating thicknesses for which the approximate theory presented in the appendix is adequate for describing the time evolution of temperature rises. The results of this calculation show that for thin coatings (about 10 microns thickness) the approximate theory should hold for time intervals up to 100 μsec whereas for the relatively thick coatings used in this study (about 56 microns) the approximate theory should be valid for time intervals up to a millisecond.

4. Optical Measurements of Oxide Cathodes

C. A. Stolte

Photoelectric yield and thermionic pulse emission data have been obtained from a passive-based BaO coating. This cathode, PL2BB1, was mounted in the structure shown in Fig. 12 of the previous report. This structure was designed so that the cathode can be cooled to near liquid nitrogen temperature. The cathode coating was prepared in the same way, and was converted using the same schedule, as the active-based cathode, PL2FF1, mounted in the same structure. The details of the preparation and conversion schedules are given in Scientific Report No. 4 of this series.

The pulse emission after conversion of PL2BB1 was less than 5 mA/cm^2 compared to 185 mA/cm^2 obtained from PL2FF1 after its conversion. The thermionic pulse emission, J_s, as a function of hours life at 800°C is shown in Fig. 7. The emission

after 24 hours life was 50 mA/cm^2 compared to 1.6 amp/cm^2 obtained after 2 hours life from the active-based cathode PL2FF1.

The photoemission yield obtained during this interval was low and exhibited a large amount of scatter. The magnitude of the yield at a given photon energy, with constant light intensity, was also erratic. This erratic behavior did not appear to be associated with the yield from the cathode but rather to be a consequence of the measuring technique.

After 24 hours life the cathode was operated with the current drain indicated in Fig. 7 in order to activate the cathode so that the source of the erratic behavior could be determined. The thermionic pulse emission after 20 hours of current drain had increased from 0.05 to 2.98 amps/cm^2.

At the end of this life period the cathode temperature was reduced to near liquid nitrogen temperature and a photoelectric yield plot taken. The magnitude of the yield had increased several orders of magnitude as a consequence of the electrolytic activation but the erratic behavior was still present.

With the tube immersed in the boiling liquid nitrogen a "noise" signal is generated on the cathode lead which makes it impossible to measure the cathode current and as a consequence it is necessary to measure photocurrent at the Ni grid "collector". To reduce the noise appearing on the collector lead it is also necessary to place an Al foil shield, connected to ground, on the tube surrounding the cathode assembly.

The current-voltage plots shown in Fig. 8 show the effect
of this shield on the photoelectric current. Curve #1 was ob-
tained measuring the _cathode_ current with the collector voltage
positive with respect to ground. The shield potential had no
effect on the I-V curve when measuring the cathode current.
Curve #4 of Fig. B was obtained by measuring the _collector_
current with the cathode held negative with respect to ground
and the shield at ground. The potential of the collector with
respect to ground was equal to the volt-drop across the meter,
which was less than 120 millivolts. The curve shown is only
an indication of the variety of I-V plots obtainable with this
bias system. They all agree up to about 6 V but above this the
form of the curve is dependent upon the sweep rate of the cathode
voltage. For example, if the cathode voltage was increased to
8 volts and held at this potential, the anode current would
increase with time. This behavior indicates secondary emission
from the collector, possibly covered with BaO.

The effect of the shield potential can be seen by comparing
curves #2, #3 and #4 of Fig. 8. With the shield floating or
biased negatively with respect to ground, the collector current
curve is essentially the same as the cathode current curve.
These data indicate that the erratic behavior observed in the
photoemission yield plots was a consequence of secondary emission
from the Ni grid with these secondary electrons being collected
on the walls of the tube. With the shield at ground potential,
the finite leakage of the glass would tend to hold the glass

at ground potential and hence slightly positive with respect to
the collector. With the shield floating or biased negatively
with respect to ground, the glass wall will be held at a nega-
tive potential and the secondary electrons from the grid return
to the grid since it will remain the most positive element in
the structure. All future measurements using this structure
will be made with the shield biased negatively with respect to
ground.

Further measurements of the photoelectric yield and
thermionic pulse emission have been obtained from the BaO thin
film coating based on 0.024% Mg-Ni. The data from this cathode,
PM2FF1, presented in the last report, indicated an incomplete
oxidation of the Ba deposit, with the film depleting visually
in 2.5 hours life at 800°C. The film preparation procedure
was repeated, thus adding an additional BaO layer to that re-
maining on the base. The cathode was exposed to the Ba re-
evaporator for a total of 8 minutes with the re-evaporator at
600°C; see the last report for the details of this procedure.
The photoelectric yield curve obtained from this Ba deposit
had a threshold energy, as determined by a Fowler plot, of
2.48 eV compared to a threshold energy of 2.56 for the original
Ba deposit on this cathode base. The Ba deposit was oxidized
by admitting O_2 to a pressure of about 5×10^{-5} Torr while
holding the cathode at 300°C. These conditions were maintained
for 6.5 hours during this oxidation, compared to a time of

3 hours with a cathode temperature of 200°C during the initial film formation.

The tube was pumped for 24 hours, with the valve closed, to a pressure of 1×10^{-9} Torr. The film was then heated to 800°C for 4 minutes to measure the thermionic pulse emission; the emission was 0.424 amps/cm^2; this can be compared with the value of 0.152 amps/cm^2 for the first film just prior to addition of the second layer.

Curve #1 of Fig. 9 shows the final yield curve for the first BaO layer just prior to addition of the second layer. The yield curve taken after additional deposition and this brief life period is shown by curve #2 of Fig. 9. The film changed from the typical patchy multicolor appearance to a uniform grey color during the 4 minute life period.

To assure complete oxidation the film was again exposed to 5×10^{-5} Torr of O_2 with the cathode held at 300°C for 5 hours. After the pressure had been reduced to the order of 10^{-9} Torr, the pulse emission at 800°C was 0.295 amps/cm^2. The BaO film, after the brief life period required to measure the pulse emission, had a uniform light blue color with a grey-blue color in the center where the film from the original deposition remained. The yield curve obtained after this life period is shown as curve #3 of Fig. 9.

The yield curves obtained from thin film BaO coatings have a different shape and less structure than those obtained from the coatings obtained by converting $BaCO_3$. This difference is

illustrated by curve #4 of Fig. 9. This curve was obtained from cathode PL2FF1, BaO produced by converting $BaCO_3$, after 6.2 hours life at 800°C. The reason for this difference is not known at this time, but could be a consequence of the different means of producing the film coatings as opposed to the more standard coating. It is possible that the film cathode contains, from the oxidation process, a large oxygen impurity which could act as an acceptor level and hence change the photoelectric yield characteristics. The spectral reflectance of the thin film coatings would also be different from that of the porous coatings, and this could possibly change the shape of the yield curves, since the reflectance is not taken into account when computing the yield.

The photoelectric yield taken after the re-deposition and oxidation of the film, see curve #3 of Fig. 9, is down two orders of magnitude from the yield taken before the re-deposition, which is shown in curve #1 of this figure. This lends support to the postulate that excess Ba was present in the original film.

The exciton-induced emission at 3.8 eV is not as pronounced in curves #2 and #3, again indicating that the exciton-induced emission depends upon a donor level close to the conduction band. The rise in the yield curves at about 4.3 eV, see #2 and #3 of Fig. 9, has not been observed in the yield curves taken on the more standard BaO coatings, although it may have been present but masked by the larger exciton-induced emission. This is illustrated by curve #1 of this figure, where it is possible to

discern a rise at about 4.5 eV, but the exciton-induced emission starting at 3.8 eV tends to mask it.

In spite of the many questions raised by the yield curves obtained from thin film BaO coatings, it was decided to continue with the main line of investigation, namely, a determination of the thermionic pulse emission capabilities of the thin film BaO coatings and a correlation of this emission with the magnitude of the photoelectric yield.

The data taken thus far on this thin film BaO coating on 0.024% Mg-Ni base, PM2FF1, are shown in Fig. 10. In this figure are plotted the thermionic pulse emission, J_s; the photoelectric yield at 2.5 eV, η (2.5); and the photoelectric yield at 3.6 eV, η (3.6). The values of J_s were determined using the 3 μsec pulse techniques described in detail in previous reports. The values of η (2.5) and η (3.6) were obtained from total photo-electric yield plots such as those shown in Fig. 11; each yield plot was taken at room temperature about ten minutes after a life period. The numbers 1 through 18 along the bottom of the figure correspond to the numbers in the table which give an indication of the time between the life periods and any processes which occurred during the "off" time.

The data up to 2.4 hours were presented and discussed in the last report. The re-deposition and oxidation of additional Ba indicated at 3, and the further oxidation at 4, have been discussed in detail above. During the interval between 5 and 7 the bias used during the yield measurement was connected

accidentally to the anode for a period of 9 minutes at the beginning of the life period. Thus electrolytic activation could account for the rise in the emission and subsequent decay when this voltage was removed. It is observed that the thermionic pulse emission decreased drastically during the off periods indicated by 7 and 8. The yield curve obtained at point 10, after a total of 7.45 hours life at 800°C, is shown as curve #1 of Fig. 11. The shape of this curve is similar to that of curves #2 and #3 of Fig. 9 and its magnitude lies between these two curves. There is no apparent correlation between the photoemission and thermionic pulse emission in the region of Fig. 10 between numbers 5 and 10, following re-deposition of BaO.

During the period from number 10 to 12 on Fig. 10 the pulse emission increased slowly to a level of 0.1 amp/cm^2, which is still much lower than the emission observed on the standard BaO coatings on an active base after a few hours life. The photoyield curve obtained after 17.97 hours, as shown on curve #2 of Fig. 11 does reflect the increase in the thermionic pulse emission.

Photoelectric yield plots obtained during the "off" periods showed a decrease in the magnitude of the yield with time after a given life period. This has been observed in the past and, in the last report, a model was formulated which could explain the decrease with time. The model proposed was a donor diffusion model in which it was postulated that the donors formed at the surface as a consequence of chemical activation

diffused into the crystal. Therefore, in the absence of a pro-
duction mechanism, the donor concentration at the surface would
decrease and hence the photoelectric yield would decrease with
time. This model would explain the decrease of the yield with
time and the decrease of the thermionic emission during an off
period, but would not explain the low thermionic and photoelec-
tric emission observed after 18 hours life compared with the
high emission early in life. Since the BaO film and the entire
structure had been exposed to a high oxygen pressure during the
oxidation of the film it seemed possible that a competing
process, namely oxygen poisoning, could account for the low
emission. To reduce the possibility of poisoning, the anodes
used to measure the emission and the life anodes were heated to
800°C at point 12 of Fig. 10. The pressure in the tube before
the anode cleaning was 2×10^{-9} Torr and increased to 2×10^{-7}
Torr during the cleaning. The anode temperature was held at
800°C until the pressure decreased below 10^{-7} Torr; the time
required was about 20 minutes for each anode.

The effect of cleaning the anode is seen by the increase
of the thermionic emission shown in the period between points
12 and 13 of Fig. 10. This increase indicates that operation
of the cathode in the presence of the "dirty" anode kept the
emission at a low level. The photoelectric yield after this
life period, curve #3 of Fig. 11, similarly shows an increase
over the previous yield, curve #2. The decay observed during

the off period 13 indicates that the decay in yield and thermionic emission is not an anode effect.

It was considered possible that the decay during the off period was a consequence of the abnormally high background pressure. At point #14, in an attempt to reduce the background pressure, the tube was baked, using heater tapes, to a temperature of 160°C for 6 hours during which time the pressure increased to a maximum of 1.8×10^{-7} Torr and then decreased to 7×10^{-9} Torr. The tube was allowed to pump for two days after which the pressure was 1.2×10^{-9} Torr, which was essentially the same as that before the bake, and at least an order of magnitude greater than the pressure obtained in other tubes in these investigations. It appears that the metal valve attached to the tube for the oxygen admission has a leak rate such that the pressure remains above 10^{-9} Torr. The data taken after this bake, the periods between 14 and 16, indicate that the bake had no effect on the emission.

Immediately following the period from 15 to 16 a photoelectric yield plot was obtained, after which the photoelectric yield at 2.5 eV was monitored as a function of time. The yield decreased about 27% in 20 minutes; the pressure in the tube during this time was 1.5×10^{-9} Torr. To investigate the effect of increased pressure on the yield, the valve to the oxygen flask was opened and the tube pressure was increased to 7×10^{-9} Torr. The yield at 2.5 eV decreased rapidly and, after 20 seconds, was down a factor of 15 from the value before the

valve was opened. The yield at 2.5 eV remained fairly constant at the lower value after the valve was closed and the pressure reduced to about 2×10^{-9} Torr. The cathode temperature was increased to 800°C immediately after this oxygen admission and the pulse emission data between points 16 and 17 of Fig. 10 obtained. The pulse emission at the beginning of this period was higher than at the beginning of the previous life periods and the emission increased more rapidly. The photoelectric yield plot taken after this brief life period, at point 17, was essentially the same in magnitude and shape as the plot taken immediately after the preceding life period, at point 16 before the oxygen admission.

Thus it appears that the decay observed during the off periods is a donor destruction phenomenon occurring as a result of the residual pressure in the tube. The facts that the emission did not decay to zero during the brief period of oxygen admission, and the rapid increase in the emission during the life period from 16 to 17, indicate that the destruction process had not gone to completion as it apparently had in the previous cases.

The cathode was then lifed at 800°C, the period between #17 and #18, and the photoelectric yield curve #1 of Fig. 12 was obtained after this life period. The yield at 2.5 eV, monitored as a function of time after curve #1 was obtained, decreased about 17% in 12 minutes; the tube pressure was 1.5×10^{-9} Torr. The pressure in the tube was then increased by means of the

metal valve and the yield at 2.5 eV monitored as a function of time. The results are plotted in Fig. 13, where the yield at 2.5 eV and the tube pressure are plotted as functions of time. The yield at 2.5 eV decayed rapidly, with the oxygen pressure held at about 5×10^{-9} Torr, and could be fit with an exponential function with a time constant of 13 sec. Even more rapid decays have been observed following exposures to higher oxygen pressures, although in these cases no detailed measurements were obtained. These results have, however, shown that the time constant is dependent upon the pressure.

After the pressure had been reduced to 10^{-9} Torr, the photoelectric yield was measured, and is shown as curve #2 of Fig. 12. The cathode was again lifed at 800°C with the results shown in Fig. 10 after point #18. The yield curve obtained after this life period is shown as curve #3 of Fig. 12. The yield curves of Fig. 12 do reflect the changes observed in the thermionic pulse emission, however, no quantitative correlation will be attempted because of the observed decay of the photoelectric yield during the off periods.

The results plotted in Fig. 10, the photoelectric yield curves shown in Figs. 9, 11 and 12, the yield decay curve shown in Fig. 13, and the observations indicated above shed further light on the behavior of BaO. Several conclusions can be inferred from the data referred to above. First, it is apparent that the thermionic pulse emission and photoelectric emission are dependent upon the environment in the tube. This is

illustrated by the decay of the emission during the off periods, the effect of cleaning the anodes, and the oxygen admission data. Second, there is a qualitative correlation between the photoelectric yield and the thermionic pulse emission as seen in Fig. 10.

Before attempting any quantitative correlation one would have to eliminate the time dependence of the yield. Quenching the cathode to liquid nitrogen temperatures, as possible with tube PL2FF1 described above, decreases the time dependence of the yield but the decay appears to be a consequence of the tube environment as well as the temperature of the coating.

The time dependence of the yield in the thin film tube, PM2FF1, was apparently a consequence of inadequate vacuum, even at 10^{-9} Torr, rather than a donor diffusion process as postulated in the last report. Third, there is a large difference between the structure of the photoelectric yield curves observed with the thin film cathodes and the more standard BaO cathodes. This difference is not understood at this time and further investigation will be required to explain the difference.

It is apparent that any quantitative correlation between the photoelectric yield and the thermionic emission will have to be obtained by measuring the yield and the thermionic emission under identical conditions and at the same time. The use of the energy analyzer, discussed in the last report, should aid in this kind of simultaneous measurement, since it should be possible to distinguish the photoelectrons from the background thermionic emission.

The use of the electron multiplier at the output of the analyzer necessitates running the analyzer structure at 2000 volts negative with respect to ground. If the glass walls remain near ground potential, there exists a large potential between the glass wall and the analyzer box. Hence, the region inside the box near the hole used to allow illumination of the cathode (see Fig. 16 of the last report) is not a field-free region. This appears to distort the electron trajectories and to give an apparent shift in the zero of energy. This shift is dependent upon the potential of the glass wall and hence the determination of the zero of energy is not dependable.

While several energy distribution plots of thermionic and photoelectric emission have been obtained, these considerations indicate that the absolute calibration of energies (zero point) is in doubt. The use of an Al foil shield, at box potential, around the tube envelope appears to eliminate this problem. This would hold the glass wall at box potential by means of the finite conductance of the glass, as observed in tube PL2BB1 described earlier, and hence the region inside the box should remain a field-free region as required. A future solution for this problem will be to mount a metal mesh over the hole in the box to eliminate the distortion of the electron trajectories by an external field.

The associated equipment used with the analyzer will be modified to allow the generation and detection of an ac photocurrent. This will be accomplished by chopping the light and

employing an ac detection system to monitor the photocurrent. This will allow a separation of an ac photocurrent from a dc thermionic current and hence a simultaneous determination of the photoelectric yield and the thermionic emission. Development of a successful technique for simultaneously monitoring thermionic and photoelectric properties of an emitter would permit meaningful correlations, avoiding the uncertainties introduced when operating conditions are changed to permit lower temperature photoelectric studies.

5. Thickness Studies   R. J. Soukup

A series of experiments aimed at determining the influence of the oxide coating thickness on cathode parameters were continued. A tube, SH4, has been constructed using four standard cathode assemblies located in side-arms. All cathodes employed 0.024% Mg-Ni alloy bases, and all were coated with $(BaSr)CO_3$ containing a radioactive tracer of Sr^{89}. The cathodes were shaved to thicknesses which ranged from 0.0024" to 0.0038"; measured by comparing the radioactivity of the coating with that of a sample of known weight, as described in the previous report.

The structure was processed and the carbonate converted to the oxide following the procedure outlined in Scientific Report No. 2 of the previous contract.[1] The same change in procedure as discussed in the previous report (elimination of the bakeout after conversion) was made on this tube. During

[1] Contract No. AF 19(604)-3890, p. 33.

conversion one coating cracked and another peeled at the edges. No attempt was made to measure the pulsed emission from these two cathodes.

Difficulty was encountered attempting to measure the exact operating temperature of the cathodes. Thermocouples were not used because it was found that the coating would not adhere well to the base metal after the Pt-Pt + 10% Rh thermocouples were attached. During the processing procedures the glass envelope surrounding the cathodes collected a slight deposit of evaporated metal, making optical temperature measurements difficult. However, each of the two cathodes was held at a constant temperature throughout life.

Another tube structure, SH3, containing four cathodes in a common envelope was described in the previous report. The emission levels of the cathodes in tube SH4 were higher than those in SH3. A possible explanation for this, in view of the difficulties encountered in measuring the operating temperatures, may be that the cathodes in tube SH4 were at a higher operating temperature. A difference of 25°C could account for the higher emission, as can be calculated from Richardson's equation, assuming the same value for A for all cathodes, and a ϕ of 1.4 eV.

The diffusion equation for an activator from the base nickel, where the initial concentration of activator is uniform, predicts that $q = C_o (\frac{D}{\pi t})^{1/2} = kt^{-1/2}$ where q is the rate at

which activator flows through the oxide-nickel interface.[2]
Evaluating the constant k yields a more precise measure of cathode reduction than does the amount of integrated Sr evolution at one chosen time. These data are listed in Table I. The values of k are obtained by plotting the integrated Sr evolution vs. time on log-log paper and fitting to a best 1/2 slope line. In this case $Q = \int q \, dt = \int k \, t^{-1/2} \, dt = 2 \, k \, t^{1/2}$.

Also shown in Table I is the coating thickness, the final stable emission level as determined by the deviation and the 20% crossover method, and the average conductivity.

Table I

Cathode No.	Coating Thickness (mils)	Final Emission Level (A/cm^2)		Average Conductivity (Mhos/cm^2)	$k(\mu \, gm/cm^2 sec^{\frac{1}{2}})$
		J_D	J_{20}		
SH3-FF1	2.0	1.5	2.6	7×10^{-3}	3.19×10^{-3}
-FF2	3.5	3.0	6.9	9×10^{-3}	3.64×10^{-3}
-FF4	3.9	4.4	--	7×10^{-3}	3.98×10^{-3}
SH4-FF3	3.8	7.8	12.9	32×10^{-3}	66×10^{-3}
-FF4	2.4	2.7	3.7	50×10^{-3}	4.17×10^{-3}

Tube SH3 was operated through 500 hours of continuous life, and then turned off. The data obtained from these cathodes are shown in Figs. 14, 15, and 16, and include the

[2]Peterson, Anderson and Shepherd, J. Appl. Phys. 28, No. 1, 22-23, January (1957); D. A. Campbell, J. Appl. Phys. 33, No. 4, 1609-1610, April (1962).

Page 37

integrated Sr evolution, deviation and 20% saturation emission, and conductivity calculated from the deviation emission measurements. Tube SH4 was operated through 1000 hours of continuous life and then turned off. These data are shown in Figs. 17 and 18. Note that the data are plotted to the same scale on each figure except Fig. 17 where the Sr evolution scale is an order of magnitude larger.

As can be seen from the figures and from Table I, the Sr evolution rate and integrated Sr evolution are higher for cathode SH4-FF3 than would be expected. The values calculated for k for all three cathodes in tube SH3 and for cathode SH4-FF3 are of the same order of magnitude and the variations may be due to small temperature differences encountered from cathode to cathode.

The large value of k for cathode SH4-FF3 might be explained by a higher operating temperature and hence more rapid diffusion of Mg to the oxide. This diffusion system is not a simple one, since Mg is present both in solution and as an intermetallic compound. While this problem has been treated[3] by Campbell (see ref. 2), the numerical values of the effective activation energy are not well established.

According to C. W. Glewwe[3]

$$q = q_0 \exp \left(- \frac{Q + H}{2RT} \right)$$

[3]Scientific Report No. 1, "Studies on Base Nickels for Oxide-Coated Cathodes," Contract No. AF 19(604)-3890, p. 47.

where for a Mg-Ni alloy $Q = 56.6 \frac{Kcal}{mole}$ and according to the experimental results of D. A. Campbell[4] H is approximately 28 $\frac{Kcal}{mole}$ Using these values a temperature difference between cathodes in tube SH3 and cathode SH4-FF3, sufficient to explain the difference in Sr evolution, would have to be about 72°K. This large a temperature difference seems improbable.

A new tube containing four cathodes of different thicknesses is being constructed and further studies of this problem will be continued.

[4]Scientific Report No. 1, Contract No. AF 19(604)-3890, p. 32.

III. Studies of Non-Thermionic Electron Sources

1. Introduction

Thermionic emitters are characterized in general as those in which the necessary energy required for electron escape at the surface is supplied thermally. The electron energy distribution in the emitter is in thermal equilibrium with the lattice, and only that portion of the electron population having surface-directed energies equal to or greater than the thermionic work function can escape. In addition to thermal excitation, it is possible to supply excess kinetic energy to electrons in a solid so that these "hot electrons" can escape.

To show promise of providing a useful electron source, any non-thermionic emitter should satisfy a number of criteria. These include the following:

a) The current density, and total current per device, must be adequate.

b) The excitation energy should not be too difficult to supply, in comparison with thermionic excitation.

c) The velocity distribution of the emitted electrons must be limited to facilitate focusing, modulation, and other utilization requirements.

d) Random fluctuations, or noise, must be limited.

e) Lifetime of the source, in its projected application and environment, must be adequate.

The above list is not exhaustive, and the relative importance of each criterion will of course depend upon the projected application.

In the studies being undertaken by this project, two
general means of exciting the electrons are being considered.
In both, the excitation energy will be in the form of externally
applied electric fields (as in normal field emission). One
scheme involves the acceleration of electrons while passing
through a thin film insulator and the second involves the co-
operative acceleration of electrons in a superconductor.

The first of these two emission mechanisms requires elec-
tron tunneling through a thin insulating film and subsequent
penetration of a thin metal overlayer into vacuum.* Devices to
observe these phenomena consist of a metal base, a thin in-
sulating film (of the order of 100 $\overset{o}{A}$), and a thin metal over-
layer. When a potential of a few volts is applied between the
metal layers an electric field of the order of 10^7 volts/cm is
established in the insulating film. Fields of this magnitude
are large enough to cause field emission of electrons from the
negative metal through the potential barrier of the insulator
into the positive metal film. If now this metal film is thin
enough an appreciable fraction of the electrons may be able to
reach the metal vacuum interface with energy greater than the
work function and pass into the vacuum. This last requirement
implies that the thickness of the insulator be chosen such
that a voltage greater than the metal-vacuum work function can
be applied before sample damage or breakdown occurs.

*C. A. Mead, Proc. IRE 48, 359, March (1960).

The possibility of obtaining enhanced emission from a superconducting field emitter has also been established. It is argued that, if a superconductor is made to operate under conditions approaching those which would return it to the normal state, the density of coupled electrons carrying current in the bulk of the material will approach zero. As a consequence, the surface-directed kinetic energy of these electrons will permit their escape over the barrier without tunneling. Experimental results have been presented for Nb and Ta emitters which show that the I-V characteristic of a superconducting field emission diode passes through a negative-resistance region as the emitting tip makes a transition to the normal state. The existence of such a negative-resistance region is predicted by the model in which the emission enhancement occurs as a consequence of "hot" electrons passing over the potential barrier rather than tunneling through it.

    2.   <u>Thin Film Dielectric Studies</u>   O. L. Nelson

        A. BeO and Al_2O_3 Systems

Studies of thin film metal-oxide-metal tunnel current devices have been continued, with emphasis placed on the properties of the insulating oxide layer. The sample configuration used is that of a metal-insulator-metal sandwich, as discussed in preceding reports of this series. Previous samples have contained oxide films which were formed by anodizing the vacuum-deposited metal underlayer in ammonium tartrate at pH 5.5. Al_2O_3 films formed in this manner yielded results which could

be matched to the Fowler-Nordheim tunnel current equation, but which showed polarization and aging effects. The BeO films formed by anodizing did not in general obey a simple tunnel current equation.

In an attempt to determine what effect the method of oxidation has on the properties of the oxide, other methods of oxide formation have been tried.

One such method is heating the metal underlayer in an oxygen atmosphere. Samples Be-9 and 10, discussed in the previous report, were heated in an oxygen flow at one atmosphere pressure for 1 hour at 200°C and for 1.7 hours at 110°C respectively. After the metal overlayers were deposited, measurements showed that all active areas of both samples were initially shorted.

These results indicate that the times and temperatures used were insufficient to form a continuous film. However, to check whether the heating would cause diffusion of the underlayer metal into the oxide, a series of four samples were prepared. Underlayers for Be-11, 12, 13 and 14 were simultaneously deposited, and the oxide films were formed as follows: Be-11 was anodized (in ammonium tartrate) at 3.9 V for 6 minutes. Be-12 was anodized at 3.9 V for 6 minutes and then baked at 310°C for 130 minutes in an O_2 atmosphere. Be-13 was anodized at 5.8 V for 7 minutes. Be-14 was not anodized, but was baked at 310°C for 130 minutes in O_2. Nine metal overlayers were deposited on each sample; numbers 1-5 were Al and 6-9 were Au.

Unfortunately, Be-11 was damaged in mounting for overlayer evaporation and the controlled comparison (between Be-11 and 12) is thus lacking.

Be-12 showed all active areas shorted except overlayer #7 which had a 220 kΩ slope at the origin and showed curvature at higher currents. Be-13 had two shorted areas, 1 and 5. The rest showed, at least qualitatively, tunnel current characteristics, although the current levels were held quite low to avoid breakdown. Be-14 had four shorted areas; four areas which had resistive characteristics of about 100 kΩ , and one, overlayer 7, which had a slope of 2×10^6 ohms at the origin with curvature at higher currents.

These results suggest that heating in O_2 for 2 hours at 310°C may be detrimental to oxide films already formed (BE-12), and does not form a good oxide film (Be-14). Sample Be-13 indicates that anodizing is, however, a possible technique.

One more Be sample, Be-15, and one Al sample, Al-30, were heated in O_2 at 360°C for 3.5 hours. Al and Au overlayers were deposited, and I-V characteristics were obtained. Al-30 showed all active areas initially shorted. Be-15 contained seven shorted areas, one with a resistive slope of 40 kΩ , and one which had a resistive slope of about 1 megohm, with curvature at higher currents.

The preceding results indicate that the described technique of baking the underlayer in an O_2 atmosphere is unsatisfactory for forming oxide films for tunnel current samples. Another

possible method of oxide formation is bombardment of the metal underlayer with oxygen ions. A vacuum tube structure was constructed for this experiment which consisted of a high vacuum valve, holders for the samples, and a hot cathode plasma discharge chamber. As shown in Fig. 19, the discharge was sustained by a heated W ribbon electron source with an electrode configuration so arranged, with an axial magnetic field, that the electrons were confined to a region of approximately 1 inch length and 1/4" diameter. Ions were extracted by a grid parallel to the magnetic field axis and the samples were mounted behind this grid. O_2 was introduced to a chamber behind the valve by means of a break-in tip from a cylinder of pressurized O_2. The break-in tip was then resealed.

After preliminary processing, two samples were inserted, Be-17 and Al-31. The plasma was established at an O_2 pressure of 1.4×10^{-3} Torr, with 60 V anode potential and a total current of 100 mA (the magnetic field was about 1500 gauss). The underlayer of Be-17 was biased 6 V negative with respect to the anode potential (which is assumed also to be the plasma potential) for 13 minutes. The ion current collected by the sample and holder was 5 μA. Al-31 was left floating at plasma potential.

The W filament temperature was then increased so that, at the same O_2 pressure, the plasma was stable at 40 V and 250 μA. Al-31 was biased 6 V negative with respect to the anode potential for 20 minutes, and drew 9 μA ion current. During this period Be-17 was left floating.

Prior to oxygen ion bombardment, Al-31 had been stored in a dust-tight container for 6 weeks, and Be-17 had been stored for 4 weeks. Au and Al overlayers were vacuum deposited on these samples and also on Be-16 and Al-32. Be-16 had simply been stored with Be-17, and Al-32 had been stored with Al-31, with no further attempts at oxide formation. Table I summarizes the results from the initial I-V characteristics.

Table I

VOLTAGE REQUIRED TO PASS 10 µA CURRENT, OVERLAYER POSITIVE

Sample	Overlayer #								
	1	2	3	4	5	6	7	8	9
Be-16	0	0	0	0	.06	.03	0	.02	.02
Be-17	0	.02	0	0	0	.03	.02	0	.02
Al-31	0	.14	0	0	.12	0	.25	1.0	0
Al-32	0	0	0	0	0	.02	.03	.04	0

All of the non-shorted active areas were resistive at the origin, the resistance value being given by the indicated voltage divided by 10 µA, except Al-31 overlayer 8. This active area yielded an I-V curve which qualitatively follows the tunnel current characteristic. A Fowler-Nordheim plot, however, yielded curved lines whose sloped changed by a factor of two over only 1 decade of current. The values of the slope, V_o, were of the order of 5 V. Al samples which have an anodically formed oxide

film typically match the Fowler-Nordheim equation quite well, and have values of V_o of the order of 10 times the forming potential.

The results obtained from the first oxygen-ion-bombarded samples were not encouraging; however, two more samples were made. Al-33 and Al-34 were bombarded for 30 minutes with 12 V dc bias, from a plasma sustained at 1.3×10^{-3} Torr O_2 pressure with 45 V and 100 mA. When these samples were measured all active areas were initially shorted.

Applying a dc bias to the samples which is higher than the breakdown voltage for a partially formed oxide may cause continued breakdown of the oxide film as it forms. If an ac bias is used the constant high field relaxes during the cycle but a net dc bias may still be maintained because of the rectification effect of the ion transfer. Accordingly, a sample which had been stored in a container for 4 weeks, Al-35, was biased at 8 V rms, 60 cps, with respect to the plasma anode potential, for 45 minutes. The O_2 pressure was 1.2×10^{-3} Torr and the plasma was sustained at 160 mA with 42 V anode potential. Overlayers were deposited on Al-35 and also Al-36, which had been stored with Al-35. I-V characteristics were obtained which showed all active areas on both samples to be shorted.

Although all samples for which the oxidation of the underlayer was attempted by oxygen ion bombardment were shorted, or resistive, this may have been the result of some other factor. A further attempt, with comparison samples, will be made.

Because of the possibility of polarization-induced field
changes in the insulating oxide films in tunnel current samples,
it is not unexpected that the I-V characteristics change as a
function of time when a fixed voltage is applied. Examples of
this behavior have been presented in earlier reports of this
series. To obtain more detailed information on these polariza-
tion phenomena, a measuring system has been constructed to de-
termine the complex impedance of the sample as a function of
time. This is done by superimposing a constant ac voltage of
small amplitude on the dc bias voltage applied to the sample.
The ac component of the current is then monitored, and the mag-
nitude of this current and also the phase shift with respect to
the applied voltage are plotted as a function of time. A block
diagram of the system is shown in Fig. 20.

The dc response is measured with a four probe technique.
The voltage is measured using a high impedance electrometer
voltmeter, the output of which can be applied to an X-Y recorder.
The dc bias is provided by a regulated variable dc power supply
with an internal impedance of less than 0.01 ohm. The constant
ac voltage (20 mV, 100 to 1000 cps) is applied across a 6 ohm
resistor in series with the sample and dc supply. The current
is sampled by a series resistor which can be selected as 0, 10,
100 or 1000 ohms. The dc component is applied directly to the
Y channel of the X-Y recorder. The ac component is amplified,
with the small power supply ripple and pickup noise cancelled
in the differential amplifier, and applied to a phase meter for

comparison with the applied ac voltage. A signal proportional
to the half-cycle average value of the ac current is recorded
on one channel of a time base recorder, and the phase shift is
plotted on the other channel. The X-Y recorder can also be
operated in the T-Y mode to plot dc current as a function of
time.

Not all of the equipment has been obtained as yet, but
preliminary calibrations and results have been obtained using
temporary equipment. These preliminary results indicate that
the circuit performs satisfactorily and, as an example, one set
of data is presented from sample Al-10. This sample contains a
50 $\overset{\circ}{A}$ Al_2O_3 film formed by anodizing in ammonium tartrate at
4 V for 4 minutes. This sample has been discussed previously
in Scientific Report 3.

Figure 21a shows the I-V characteristic from Al-10, #3
overlayer negative, and Fig. 21b shows the concurrently obtained
ac current and phase angle as functions of time. The ac signal
applied was 0.02 V rms at 400 cps. The current sampling re-
sistance was 100 ohms. The phase shift obtained with the sample
replaced by a resistor was less than 1°, which was about the
minimum detectable phase shift with the particular equipment
used. The ac current and phase were used to calculate values
of C and G(= 1/R) for an equivalent parallel R-C representation
of the sample. These are shown in Fig. 22. Note that the ef-
fective capacitance of the sample changes as a function of time
at a fixed dc bias by greater than 10%, and shows rapid changes

when the bias is changed. The conductance of the sample decreases with time at a fixed bias, as is indicated by the dc characteristics.

Three values of the slope of the dc I-V characteristic are shown for comparison and are seen to agree quite well with the ac, or differential, conductance.

The value of the capacitance at zero bias is about 0.04 μF. Using the physical area of the sample and an oxide thickness of 50 $\overset{o}{A}$, the plane parallel plate capacitance is 0.0057 x ε_r microfarads, where ε_r is the relative dielectric constant. From the measured value of C, ε_r would need to equal 7, which is within the range of 4.5 - 8.4 quoted in the Handbook of Chemistry and Physics for alumina.

From these results it is seen that the effective parallel capacitance, as well as the ac conductance of the tunneling sample, is a function of time and of the dc bias. The static value of capacitance agrees favorably with the theoretical value. Measurements of the complex impedance will be continued when the necessary equipment is obtained.

B. MgO Systems   E. D. Savoye

MgO is an excellent insulating material with a band-gap of approximately 10 eV and an electron affinity of the order of one eV. These properties recommend its use as the insulating layer in thin-film tunneling devices; unfortunately, the attempts to produce a thin insulating film of MgO have not been successful.*

*Scientific Report No. 3 of this series, section III-A.

During the present interval the possibility of producing thin insulating layers of MgO by a sputtering technique has been investigated. The tube structure which has been designed and constructed for this purpose is shown in Fig. 23. A Granville-Phillips high-vacuum valve is used to admit argon gas to the tube structure and to control the pressure during sputtering. A hot W filament is included to supply electrons to the plasma discharge and to permit operation in a low-pressure mode. The electrons emitted from the filament are accelerated toward the first anode ring and, upon passing through the center hole in the ring, enter a field-free region between the anode rings. Those electrons which pass completely through this region are turned back by the end plate, which is held at filament potential, and re-enter the anode region. An axial magnetic field of 80 to 300 gauss is employed to confine the electron flow to the region near the axis, effectively preventing electrons from reaching the anode until they have suffered inelastic collisions with argon atoms. This process greatly increases the probability of ionizing collisions, and contributes to an enhanced plasma density at low pressures. The material to be sputtered (target material) is located between the anode rings, and is held at a negative potential to extract positive ions from the plasma.

Under typical operating conditions for this tube, an anode current of 0.5 amps is drawn at an anode voltage of 30 volts, with an argon pressure of 5×10^{-4} Torr. An ion current of 1.2 mA is drawn to the sputtering target at -770 volts. The

mean free path for argon atoms at this pressure is about 12 cm,
and the spacing between the sputtering target and the substrate
is about 6 cm. Thus by using a low argon pressure to sustain
the discharge, the sputtered atoms, on the average, arrive at
the substrate without interaction with the argon gas.

The tube structure for the sputtering studies was sub-
jected to a pre-processing schedule before any samples were made.
The tube was evacuated with a Ti sputter-pump and baked at
450°C for 14 hours. All metal parts were outgassed, using rf
induction heating. A Ti flash-filament located beyond the high-
vacuum valve was outgassed with the valve opened. A thin layer
of Ti metal was then evaporated from the flash-filament onto the
glass envelope, to provide gettering action for removing any
active impurities in the argon gas, and the valve was immediately
closed. Argon, to a pressure of one atmosphere, was admitted
through a break-in tip on the Ti flash-filament envelope. Argon
could then be admitted to the sputtering tube at controlled
pressures by means of the high vacuum valve.

Preliminary attempts were made with this tube structure to
prepare thin-film Au-MgO-Au "sandwich" devices, in which each
of the layers was formed by a sputtering process. Sputtering
of the MgO was accomplished by the use of an ac technique. An
MgO single-crystal target was mounted on a flat Ta metal plate,
and held in place inside a Ta shield by small Ta clamps. The
shield and clamps were held at anode (ground) potential during
the sputtering process, while an rf voltage of about 500 volts

peak-to-peak was applied to the metal back plate. The mobility
of electrons in the plasma is much greater than that of the ions,
and therefore the positive charge transported to the crystal by
ion bombardment during part of the rf cycle is readily neutralized
by electrons. As a result, the crystal is bombarded by positive
ions during part of each cycle, leading to sputtering of the
insulating material.

Sputtering of insulators under ac conditions has not to
our knowledge been studied in detail, and no information as to
sputtering rates is available in the literature. In consequence,
a procedure was adopted for these experiments, in which the
sputtering parameters were systematically varied in an attempt
to produce insulating thin films. Measurement of the thickness
of any successful films by, for instance, a capacitance technique,
would then provide the necessary information on sputtering rates.

The circuits used for sputtering metals and insulators are
shown in Fig. 24. The procedure was the following:

(1) A gold strip, of 0.050" width and a few thousand $\overset{o}{A}$
in thickness, was sputter-deposited onto the substrate through
a suitable mask.

(2) With the mask removed, MgO was sputtered, according
to a selected voltage-time schedule, using the rf technique
described above.

(3) Two gold overlayer strips, 0.050" wide, were sputter-
deposited through a second mask at right angles to the first
gold strip, thus forming two "sandwich" devices, in the overlaping

areas. After deposition of the final Au layers, the samples were removed from the sputter system and electrical connections were made to both ends of each Au strip.

A total of five Au-MgO-Au samples have been produced, using the above procedure upon polished glass substrates and on MgO single-crystal substrates. In all cases the samples have been found to be shorted out when first measured. However, further measurements were made, using a small spherical Au probe in mechanical contact with the MgO film in an area not covered with Au as one electrode, and the Au overlayer strip as the second electrode. The results of these probe measurements are summarized in Table I below. It should be remarked that if the Au probe was allowed to touch an overlayer, a short-circuit was always observed. This observation indicates that the probe results were not a consequence of any contamination present on either the probe or the sample.

The results of the probe measurements with MgO -2, 3 and 4 show that the films produced by sputtering MgO were insulating. However, the sandwich devices produced by sputtering overlayers onto the insulating films were shorted out. This behavior suggests that the MgO-sputtered layers, although insulating, are not continuous, i.e., there are pin-holes in the films.

In view of this observation, it was decided to sputter-deposit a fairly thick layer of insulator, and then to reduce the thickness by sputtering off a fraction of the film, using the rf technique. Sputtering from a film of non-uniform

Table I

Sample No.	Substrate	Insulator Deposition Data			Probe Measurement Results
		time (min.)	rf voltage (p - p)	freq. (Mc)	
MgO - 1	MgO crystal	13	2230*	4.9	shorted
MgO - 2	fire-polished glass	81	2830	4.9	insulating to 100 V
MgO - 3	fire-polished glass	82 83	700 1400	4.9 4.9	insulating; $R = 3 \times 10^{11}$ ohms to 12.0 V, and 6×10^9 ohms at 55 V.
MgO - 4	fire-polished glass	32	500	4.9	breakdown at 28 volts, insulating for smaller voltages.
MgO - 5	MgO crystal	Sputter "to" and "from" substrate crystal as follows:			
	a)"from";	12	1000	3.9	partial breakdown at 15-20 V, insulating for smaller voltages. Voltages up to 45V applied without definite breakdown.
	b) Au ; underlayer sputter-deposited				
	c) "to";	30	500	4.9	
	d)"from";	3	500	3.9	
	e) "to";	32	500	4.9	
	f)"from";	3	500	3.9	
	g) "to";	32	500	4.9	
	h)"from";	1.0	500	3.9	

*Sputtered without using a series capacitance.

thickness might be expected to reduce the thickness of raised areas preferentially, if the sputtering process itself is one of momentum transfer. One sample, MgO-5, has been produced using this cyclic sputtering technique, with the results indicated in Table I above. MgO-5 also was found to be shorted out when first measured, and it is seen from Table I that the probe measurements gave results similar to those obtained from the other samples.

Although successful sandwich devices have not as yet been prepared with these insulator-sputtering techniques, insulating films have been produced, as indicated by the probe measurements. During the next interval, several methods of eliminating the pin-hole problem will be investigated.

C.   Ta-Ta$_2$O$_5$-M Systems   E. D. Savoye

The sputtering techniques which have been developed have also been applied to produce Ta metal films, on glass substrates, as bases for Ta-Ta$_2$O$_5$-M sandwich devices. The method of fabrication was similar to that used in the preparation of tunneling samples from vacuum-deposited Ta films. Strips of Ta metal 0.020" wide and an estimated thickness of 10,000 Å were sputter-deposited onto fire-polished glass slides. A thin Ta$_2$O$_5$ layer of the desired thickness was formed on each strip by anodizing in a 3% solution of tartaric acid, adjusted to pH 5.5 with NH$_4$OH. Au strips 0.050" wide were vacuum-deposited at right angles to the Ta strip, and electrical connections were made to both ends of the Au and Ta strips by means of Ag paint.

Typical I-V characteristics obtained from $Ta-Ta_2O_5-Au$ samples prepared from sputter-deposited Ta are shown in Fig. 25. These results are very similar to those obtained both from vacuum-deposited Ta samples and from electropolished Ta metal sheet samples.

In order to facilitate more detailed comparisons between the several types of sample, the following analysis is presented. The Fowler-Nordheim field-emission equation can be written

$$j = j_o \left(\frac{E}{E_o}\right)^2 e^{-E_o/E} \quad ,$$

where j is the current density, E is the applied field, and j_o and E_o are constants characterizing the materials. It is seen that the current density j depends only on the applied field E for given sample materials. This circumstance affords a simple method of comparing samples composed of identical materials, but which have different oxide thicknesses: A particular value of the current density j', is chosen. Under the assumption of identical sample materials, a field of magnitude E' would exist in each of the samples when the current density j' is drawn. Assuming that $E = \frac{V}{d}$, where V is the applied voltage and d is the oxide thickness; we have E' = V'/d, where V' is the voltage required to obtain current density j' in a sample of oxide thickness d. The oxide layers are formed anodically, and there exists a linear relationship between the voltage V_A, applied to the anodizing bath, and d, the oxide thickness,* that is;

*L. Holland, "Vacuum Deposition of Thin Films," Chapman and Hall Ltd., 1956, p. 517.

$d = KV_A$, where K is the constant of proportionality. Under the above assumptions, one can write

$$V' = E'd = E'KV_A$$

or

$$\log V' = \log(E'K) + \log V_A$$

If the I-V characteristics of the samples all obey the Fowler-Nordheim relationship, a plot of $\log V'$ vs. $\log V_A$ would then be expected to fit a straight line of unity slope. The results previously obtained with $Ta\text{-}Ta_2O_5\text{-}M$ samples have indicated that the current transfer mechanism in these devices is one of temperature-field (T-F) emission,* and that the I-V characteristics do not fit the Fowler-Nordheim field emission equation except at reduced temperatures, of the order of 77°K. Unfortunately, only a limited amount of low-temperature data are available from some of the early Ta samples, however, all available data taken at 77°K have been collected and are discussed in the following paragraphs.

Three distinct methods of preparing Ta substrates for $Ta\text{-}Ta_2O_5\text{-}M$ samples have been studied: (1) vacuum-deposition of Ta upon a polished glass substrate held at 77°K, (2) electropolishing of Ta metal sheet, and (3) sputtering of Ta, in argon

*Scientific Report No. 3 of this series, section II-C.

gas at low pressures, onto polished glass at its equilibrium
temperature in the discharge tube. Ta_2O_5 layers were formed in
all cases by anodizing the Ta metal in 3% tartaric acid adjusted
to pH 5.5 with NH_4OH. The data obtained at 77°K from these
three types of $Ta-Ta_2O_5-M$ samples are collected in Figs. 26, 27,
28, and 29. As discussed above, the data are presented for
comparative purposes in the form of plots of log V' vs. log V_A,
where V' is the voltage required to obtain a current density
equal to 10 milliamps per cm^2 and V_A is the anodizing voltage.

The plots of Figs. 26 and 27 show the available data for
samples with Al overlayers biased + and - respectively. Data
are available from only two of the three types of samples dis-
cussed above, and the type of sample is noted on the figure in
each case. The limited data available for the electropolished
samples agree with those obtained from the vacuum-deposited
samples. It is seen that for both + and - polarity, a reason-
able fit to the collected data is obtained with a straight line
of slope unity, in agreement with the foregoing analysis. The
fact that such plots can be fit to straight lines of slope unity
gives some justification for the assumptions made in the above
analysis, and provides additional confirmation that the electron
transport process of importance in these devices is one of
electron tunneling.

In Fig. 28 is presented a plot of log V' vs. log V_A for
$Ta-Ta_2O_5-Au$ samples, with overlayers biased +. In this case
the data are not fit by a straight line of slope unity; however,

if a correction is made for the difference in work function between Ta and Au (4.12 and 4.82 eV respectively), then a reasonably good fit is obtained, as is shown by the curve of Fig. 29. No such correction should be necessary for the case of Al overlayers, because the work functions of Al and Ta are nearly the same (4.08 and 4.12 eV respectively).

If such a correction for the contact-potential difference is required for the case of Au overlayers positive, it should also be necessary in the case of Au overlayers negative. However, from the plot of Fig. 30 it is seen that the data for Au overlayers are fit reasonably well with a straight line of slope one, without a contact-potential difference correction. In fact, if such a correction is made, the data no longer fit a line of slope one. No explanation of this anomaly is offered at this time, however, the effect will be given further study. It should, however, be noted that both Figs. 28 and 29 show a reasonably good agreement between the results for the two types of samples for which data are available.

3. Hot Electron Emission from Superconductors

D. E. Lood

The experimental results obtained from the study of "hot" electron" emission from a superconducting field emitter definitely show that enhanced electron emission does occur as the transition from the superconducting to the normal state is approached.

The initial experiments employed a pulse technique which was described in Scientific Report No. 2. In these experiments the transition to the normal state was induced by temperature

variation. The results of these studies showed that a large current spike is produced in field emission from a superconductor when the transition to the normal state is approached. Subsequent experiments were conducted using the same pulse technique where the transition to the normal state was induced by applying an external magnetic field. The results of these experiments showed the same type of anomalous current spike was observed as the transition to the normal state was approached.

Variation of both the temperature and the external magnetic field have shown that this enhanced emission occurs in a very narrow critical region. The enhancement was observed on a number of samples using both Ta and Nb emitting tips.

The next series of experiments were conducted in an attempt to obtain stable dc operation in the excited mode. The first measurement circuit, using an electrostatic voltmeter, proved to be unsuitable because of the slow response time. This circuit and the method of operation was described in detail in Scientific Report No. 3. An improved measurement circuit was designed using a Tektronix type 536 X-Y oscilloscope which has a very fast response time. This improved circuit and method of operation were presented in Scientific Report No. 4. The results of these experiments showed that as the transition to the normal state is approached the superconducting field emitter acts somewhat like a "relaxation oscillator". These oscillations do however, provide further evidence that a negative resistance region in the I-V characteristic of a superconducting field emitter exists over a critical temperature range.

The theoretical model on which these studies are based may not be completely correct in detail as virtually nothing is known regarding the interactions of high energy electrons in a superconductor. However, the studies suggested by the model provide definite proof of an emission enhancement phenomenon in superconducting field emitters. Further, the phenomenon has been shown to occur only in a critical range of temperature and magnetic field associated with the transition to the normal state.

The present interval has been devoted to further measurements of the type reported above, with efforts made to secure more stable and repeatable enhanced characteristics. It appears that the critical variable is the tip temperature, which must be held just below but extremely close to the superconducting-to-normal transition value. While the observations described above have been verified repeatedly, it appears that internal thermal feedback makes stable operation of the system unattainable without major modifications in the emitter geometry or work function. Such efforts are being implemented and will be described when more complete.

IV.   Conclusions

From experimental results and the theoretical analysis of the oxide cathode presented in this report and in the corresponding section of the previous report of this series, we can draw the following conclusions:

1. Emission decay during long pulse current drain can be eliminated by the use of a "clean" anode.

2. For active cathodes operating at sufficiently high temperatures, pulse currents drawn to a "clean" anode results in an emission enhancement.

3. The emission enhancement is consistent with temperature increases at the emitting surface, which are predicted by a linearized solution to the heat equation, subject to the boundary conditions appropriate for an oxide cathode during pulsed current drain.

4. The theory of impulse thermal breakdown developed here for oxide-coated cathodes explains many of the aspects of cathode sparking.

5. The simplified theory presented in Appendix I appears to provide an adequate description of temperature increases occurring in oxide-coated cathodes during heavy current drain.

A BaO coating on a passive base can be activated by drawing dc current for a long period of time. The photoelectric yield and thermionic pulse emission from a thin film BaO coating are dependent on the environment in the tube. The photoelectric yield and thermionic emission can be decreased orders of magnitude

by the introduction of oxygen at low pressures. The emission during subsequent operation at 800°C recovers after the introduction of oxygen in the order of two hours, to essentially the same level as before the introduction of the oxygen.

The two attempted methods of oxide formation on vacuum-deposited Al and Be films by reaction with oxygen atmospheres were unsuccessful. The method which utilizes bombardment of the metal film by oxygen ions extracted from a plasma discharge still holds some promise, and further attempts will be made.

The circuit designed to monitor the complex impedance of thin film metal-insulator-metal sandwiches was found to perform satisfactorily. Preliminary measurements on an $Al-Al_2O_3-Al$ sample indicated that the effective capacitance of the sample changed as a function of dc bias and also as a function of time at a fixed bias. The effective conductance of the sample also changed, and appears to agree favorably with the instantaneous slope of the dc I-V characteristics.

Insulating films can be produced by inert-gas sputtering of MgO; however, further investigation is required to eliminate the problem of pin-holes in the film.

Results obtained at 77°K from $Ta-Ta_2O_5-M$ samples prepared in several different ways were compared. The limited data available indicate: (1) good agreement between the results from samples prepared in various ways; (2) the current transfer mechanism of importance in these devices is probably electron tunneling.

V.   Appendix

1. Approximate Solution of the Heat Equation Neglecting
    all Heat Loss Terms   D. A. Campbell

It was indicated in Sec. II-3 that the numerical solution
to the heat equation subject to boundary conditions appropriate
to an oxide-coated cathode during pulsed current drain gave re-
sults which are in accord with a much simpler theory. The
simpler problem neglects heat losses resulting from thermal
radiation, emission cooling and thermal conduction. If these
losses are neglected the boundary value problem reduces to

$$\frac{dT}{dt} = \frac{J_s^2 \rho}{c \, \delta}$$

subject to

$$T(0) = T_0 \, .$$

The temperature dependence of the heat generation term is given
by

$$J^2 \rho = J^2/\sigma = A_0' \, T^{9/4} \exp \left[- (2\phi - \theta)/T \right]$$

where A_0' is a constant proportional to $n_d^{1/2}$. If it is assumed
that the temperature dependence in front of the exponential goes
as T^2 instead of $T^{9/4}$ the differential equation can be integrated
directly. This substitution is justified because the exponential
dependence on T is much stronger than the power dependence on T.
Direct integration of the equation with this modification gives

$$T = \frac{W}{\ln \left[\exp (W/T_0) - (A_0 Wt)/(c\delta) \right]}$$

where $A_0 = A_0{}' \, T_0{}^{1/4}$ and $W = (2\Phi - \Theta)$.

The critical time t_c defined by this expression would be the value of t for which the denominator goes to zero. This gives

$$t_c = \frac{c\delta \left[\exp(W/T_0) - 1 \right]}{A_0 W} \approx \frac{c\delta \, \exp (W/T_0)}{A_0 W}$$

which is in accord with the complete solution obtained numerically from the set of difference equations, since A_0 is proportional to $n_d{}^{1/2}$ and the activation energy is given by $(2\Phi - \Theta)$.

2. Outline of the Computer Program Used to Obtain the Numerical Solution Presented in Sec. II-3

In Sec. II-3 the results of a numerical solution obtained on a Contral Data Corporation 1604 Digital Computer using a Fortran Program* were presented. For completeness an outline of the calculation will be presented here.

Using the symbols defined in Sec. IV the set of difference equations solved were given by

$$T(i, j+1) = \frac{1}{2} \left[T(i+1, j) + T(i-1, j) \right] +$$

$$\frac{\Delta t \, n_d{}^{1/2} A^2 T^{5/2}(N, j) \exp\left[- 2\Phi/T(N, j) \right]}{S T^{1/4}(i, j) \exp\left[-\Theta/T(i, j) \right]} \qquad \text{(A2-1)}$$

*D. D. McCracken, "A Guide to Fortran Programming," John Wiley and Sons, Inc., New York and London (1961).

subject to

$$T(1,j) = T_o \tag{A2-2}$$

$$T(i,1) = T_o - H(o)iL/(N-1)k \tag{A2-3}$$

$$T(N,j) = T(N-1,j) - \frac{L}{k(N-1)}\left[A\chi\, n_d^{1/2} T^{5/4}(N,j)\, \exp\left[-\Phi/T(N,j)\right] + \right.$$

$$\left. \beta\, T^4(N,j) \right] \tag{A2-4}$$

where Δt and N are related by $\Delta t = L^2/2k(N-1)^2$. The procedure requires calculating the values of the temperature on a lattice of points of the x, t plane, the density of points being determined by the value chosen for N. The questions of uniqueness, stability and convergence of the numerical solution have not been considered. A discussion of these questions in regard to numerical solutions of partial differential equations can be found in the mathematical literature.*

The numerical procedures are most easily outlined by a discussion in terms of the rows and column of the lattice of points in the x, t plane. The boundary condition, Eq. (A2-2), gives the value of temperature on all points in column 1 (x = o) in the x, t plane. Similarly the initial condition, Eq. (A2-3), gives

*H. W. Emmons, "The Numerical Solution of Partial Differential Equations," Quart. Applied Math. 2, 173 (1940).

G. G. O'Brien, M. A. Hyman and S. Kaplan, "A Study of the Numerical Solution of Partial Differential Equations," J. Math. Phys. 29, 223 (1951).

the value of temperature on all points in row 1(t = o) in the x, t

plane. Finally, Eq. (A2-4) relates the temperature at the Nth point

(x = L) in any given row to that of the $(N-1)^{th}$ point in the same

row.

Outline of program:

1. Calculation

1.1 Calculate T (2,2) using Eq. (A2-1) and the

values of T(1,1), T(2,1) T(3,1) and T(N,1), given

by Eqs. (A2-2) and (A2-3).

1.2 Calculate T(3,2) using Eq. (A2-1) and the

values of T(2,1), T(3,1) T(4,1) and T(N,1), also

given by Eqs. (A2-2) and (A2-3).

1.3 Repeat procedure until the temperature on

(2,2) through (N-1,2) has been calculated.

1.4 Calculate T(N,2) using the transcendental

boundary condition Eq. (A2-4). (In the program

used for this work a trial and error method was

used to obtain T(N,2) to the nearest degree Kelvin.)

1.5 Repeat steps 1,1 - 1,4 for the next row,

i.e., calculate T(2,3), T(3,3)----T(N,3).

1.6 Repeat step 1.5 for each succeeding row. In

general, one can continue the calculation until

the time corresponding to the last row calculated

(say the Mth row) exceeds the time interval of

interest. In the problem solved here, the

calculation was terminated when the calculated

value of the temperature $T(\frac{N}{2}, M)$ was greater
than 2000°K.

2. Trial and Error Scheme used in 1.4

It is first convenient to define

$$D = RHS - T(N, j)$$

where RHS is the right hand side of Eq. (A2-4). The trial and
error procedure used was to assume a value for $T(N, j)$ such that
$D > 0$. Repetitively we increase the assumed value of $T(N, j)$ by
1 degree increments until the calculated value of D becomes
negative or zero. The solution of Eq. (A2-4) was then taken
as that value of $T(N, j)$ which gave $D = 0$, or the highest value
of $T(N, j)$ which resulted in $D > 0$.

In the analysis above N was assumed to be a constant.
The value of N determines the time increment Δt (a value of
$N = 1000$ gives a value of $\Delta t \approx 0.01$ µsec). If the time interval
of interest is much larger than Δt a large number of rows must
be calculated to describe the time evolution of calculated
temperatures. To reduce the computing time required to obtain
the curves in Figs. 11 and 13 the computer was programmed so
that N would increase as the time rate of temperature change
increased hence, reducing the number of calculations necessary.

VI.   Personnel Employed on Contract

	Percent	Man Months
[1]W. G. Shepherd	10	3
D. E. Anderson	25	3
D. A. Campbell	100	3
O. L. Nelson	75	3
E. D. Savoye	75	3
R. H. Springer	100	3
C. A. Stolte	100	3
Douglas Lood	40	3
Rodney Soukup	40	3
Secretary	50	3
Engineer	15	3
Laboratory Technical Assistants		2,603 Man Hours

[1]No time charged to contract.

EXPERIMENTAL — BOMBARDMENT

0.0015" KOVAR COUNTING WINDOW

OXIDE COATING

W TROLLEY

MIRROR

VACUUM FLANGE

W FILIMENT AND HEAT SHIELD

Ti PUMP NO.2

OXYGEN SOURCE

Ti PUMP NO.1

ANODE WELLS

TROLLEY FOR INDUCTIVE HEATING OF ANODES

CONTROLLED CHEMICAL ACTIVATION TUBE STRUCTURE

OXIDE COATING BASED ON A 0.010" X 0.125" DIA. Ni DISK.

VACUUM FLANGE

4 Ni TABS

0.010" X 0.125 DIA. Ni DISK

0.005" KOVAR PARTITION

CATHODE DETAIL

FIG. 1

TEMPERATURE OBTAINED FROM NUMERICAL
SOLUTION TO HEAT EQUATION PLOTTED
AS A FUNCTION OF POSITION

FIGURE 2

PLOT OF MAXIMUM TEMPERATURE IN OXIDE COATING AS A FUNCTION
OF TIME (DATA OF FIGURE 9)

$n_o = 10^{24} \ m^{-3}$

$T_o = 1050^\circ K$

$J_o = 39 \ amps/cm^2$

TIME IN μ SEC.

T_{max} IN DEGREES KELVIN

FIGURE 4

LOG LOG PLOT OF INITIAL CURRENT DENSITY

J_o Vs n_d

T_o = 1200° K

T_o = 1100° K

T_o = 1000° K

J_o IN AMPS/CM^2

n_d = DONOR DENSITY IN m^{-3}
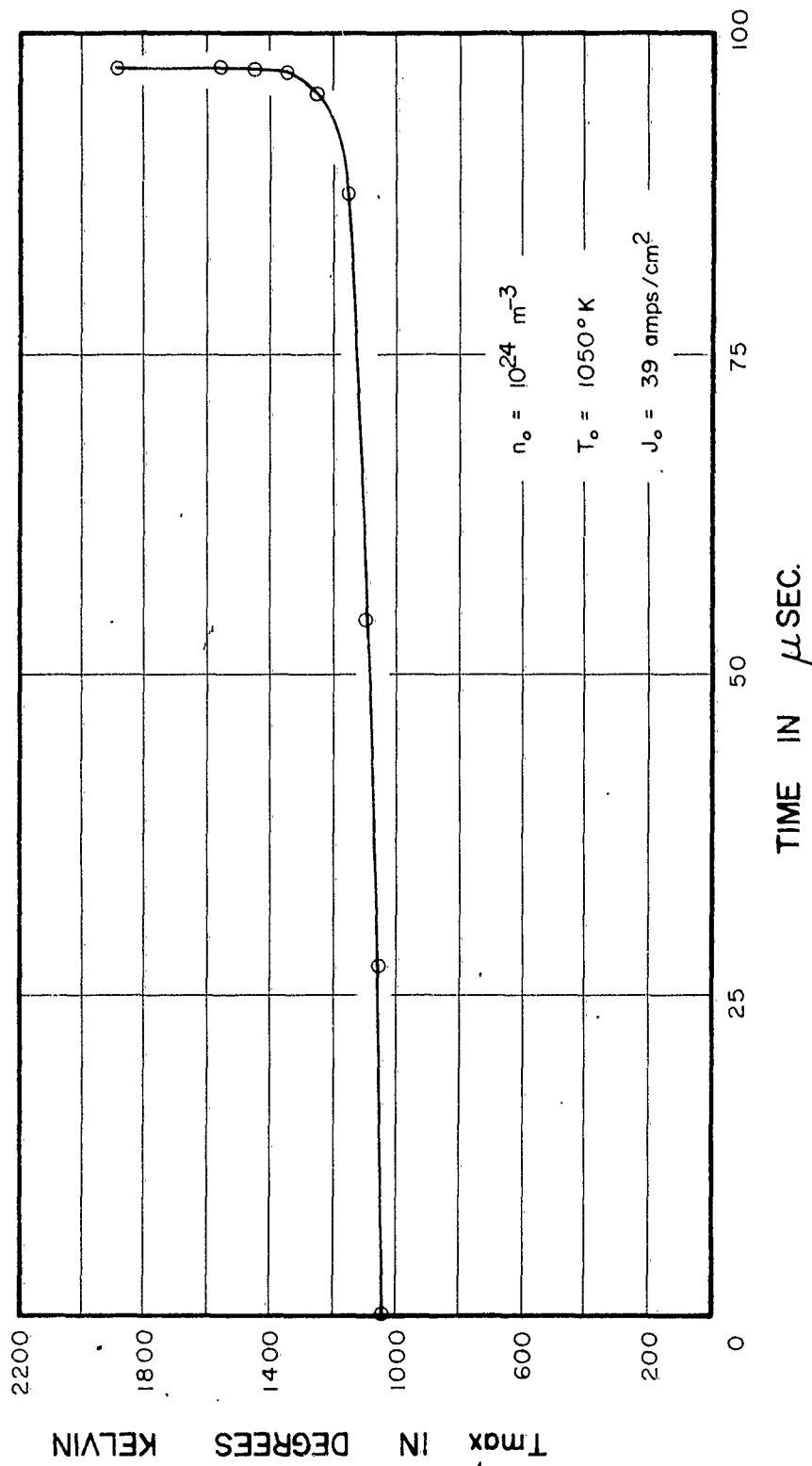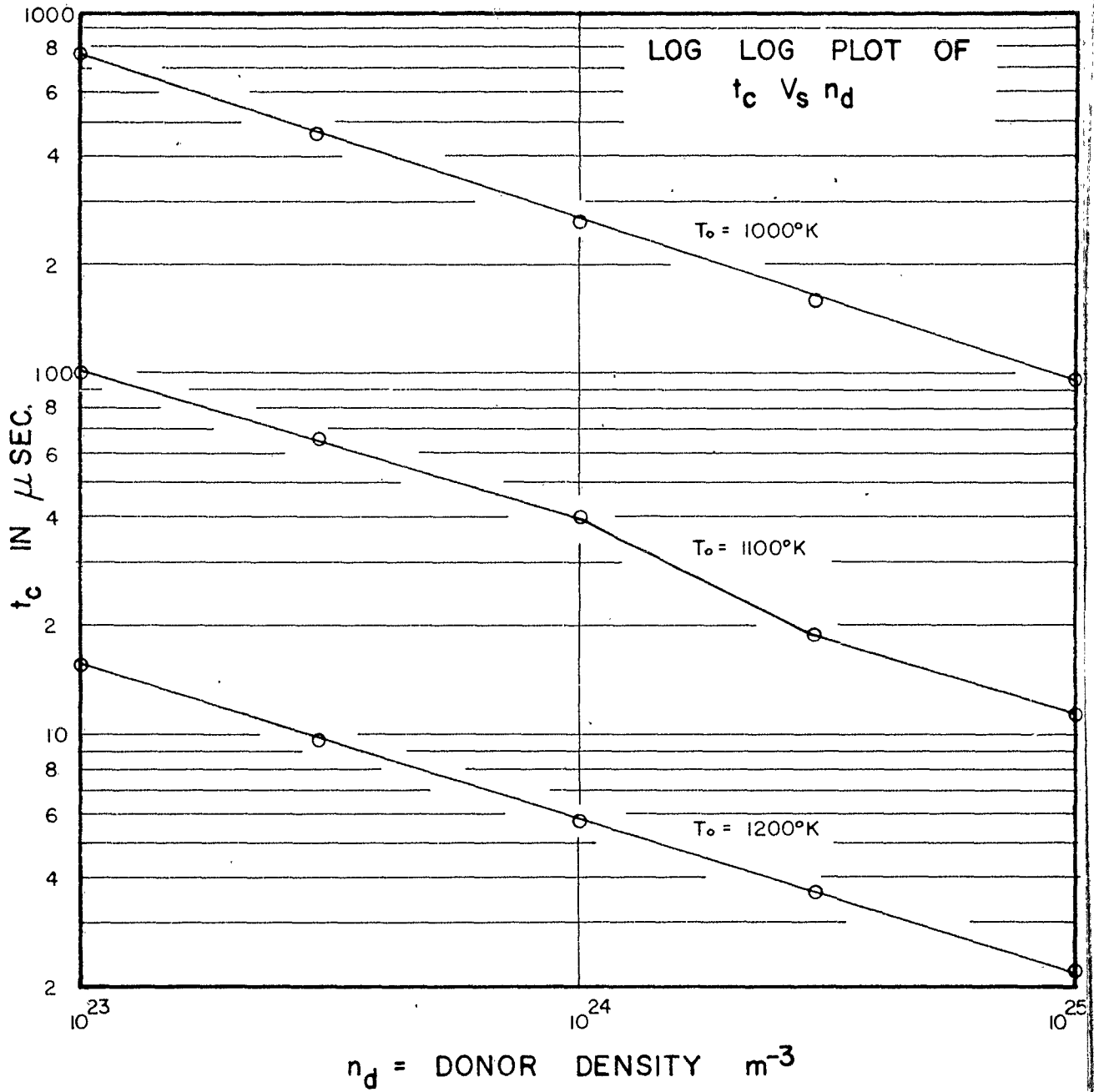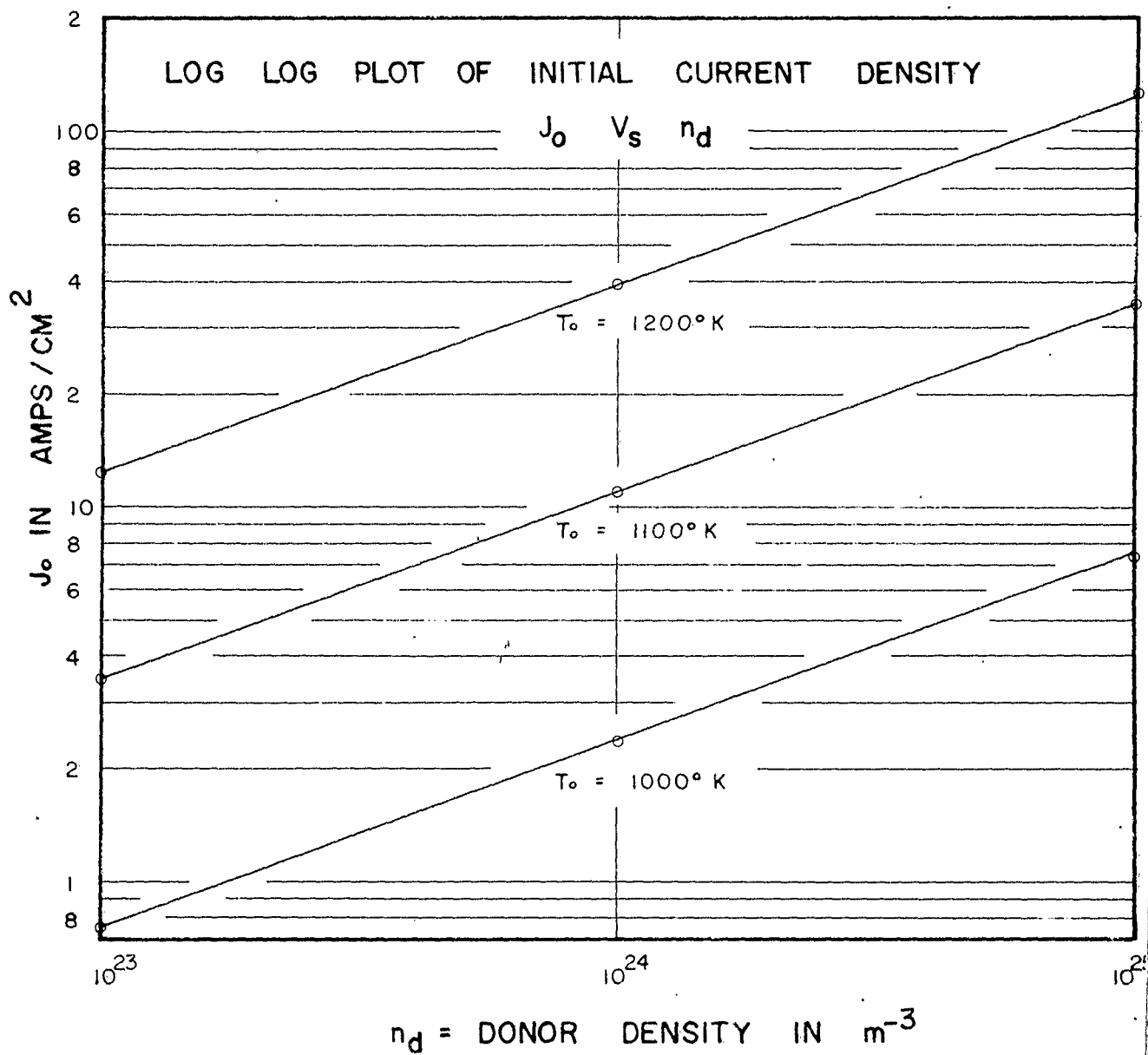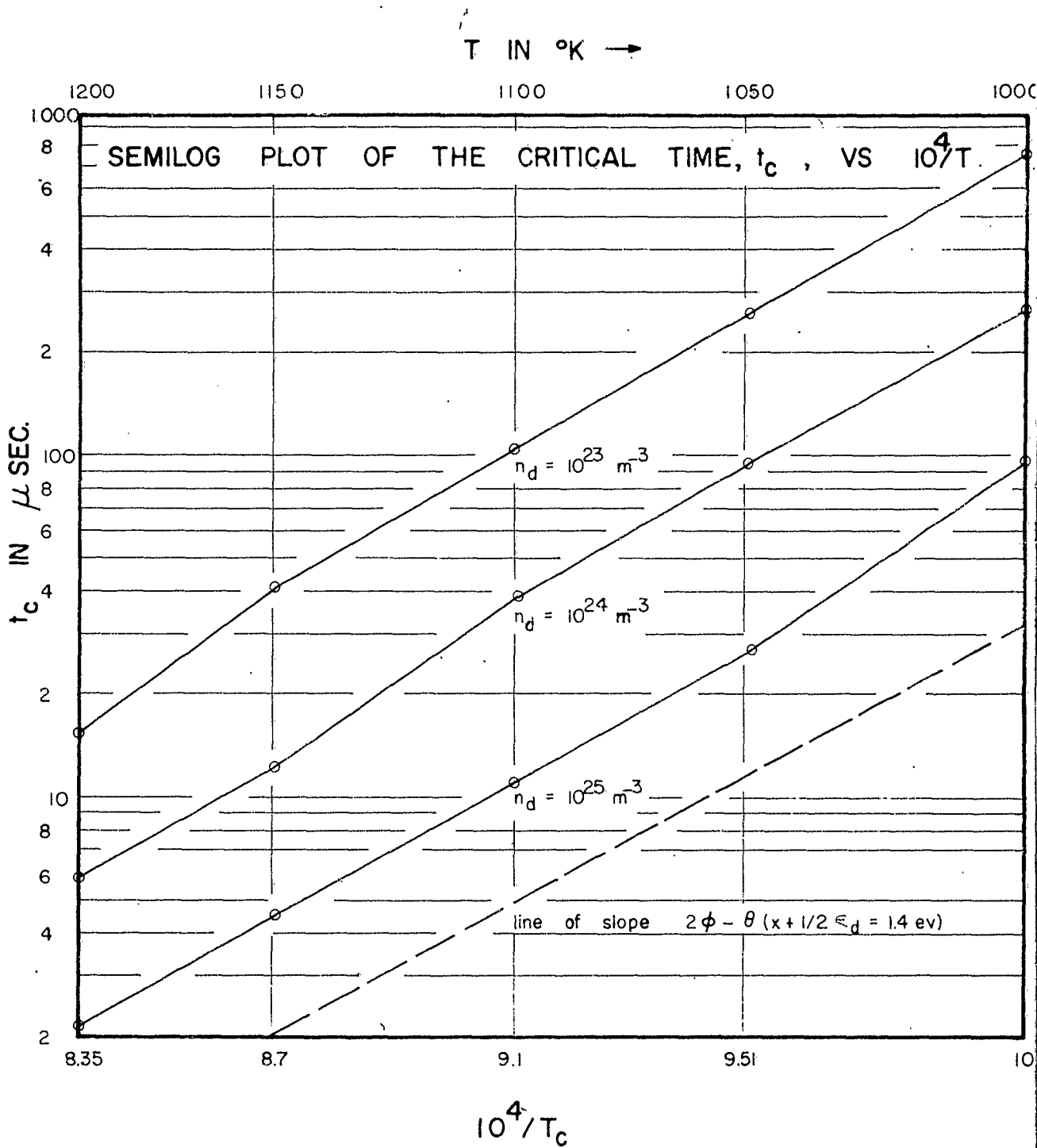
FIGURE 5

FIGURE 6

PULSE EMISSION FROM BaO ON A PURE NICKEL BASE

PL 2 BB I

ELECTROLYTIC ACTIVATION SCHEDULE:

INTERVAL	Va (D.C.)	JA (MA/CM^2)
1	24	2.2
2	10	8.4
3	50	8.4
4	100	20
5	100 → 25	20 → 71

2.98 AMPS/CM^2

Js AMPS/CM.^{2}

HOURS LIFE

FIG. 7

PHOTOEMISSION CURRENT AT 3.0 ev.vs.APPLIED

POTENTIAL FROM BaO ON A PURE

NICKEL BASE

PL 2 BB I

#1. CATHODE CURRENT
#2. COLLECTOR CURRENT
     SHIELD-85v

#3. COLLECTOR CURRENT
     SHIELD FLOATING

#4. COLLECTOR CURRENT
     SHIELD AT GROUND

CATHODE - TO - COLLECTOR (VOLTS)
POTENTIAL

I (AMPS) X 10^{11}

FIG. 8

TOTAL PHOTOELECTRIC YIELD FROM THIN FILM BaO ON A 0.024% MgNi BASE (PM2FFl)

#1 – 2.40 hrs. life at 800°C

#2 – 2.47 hrs. life at 800°C

#3 – 2.58 hrs. life at 800°C

#4 – tube (PL2FFl) 6.2 hrs. life at 800°C

PHOTOELECTRONS / QUANTUM

PHOTON ENERGY hv (ev)

FIGURE 9

PULSE EMISSION AND PHOTOELECTRIC YIELD FROM
THIN FILM BaO ON A 0.024% MgNi BASE (PM2FFI)

1 — off 24 hrs.
2 — off 26 hrs.
3 — Ba + O_2
4 — O_2
5 — off 23 hrs.
6 — 22.5^V on anode ~ 9 min.
7 — off 70 hrs.
8 — off 69 hrs.
9 — off 20 hrs.

10 — off 74 min.
11 — off 45 hrs.
12 — off 114 hrs. + RF anodes
13 — off 13 days
14 — off 11 days + 150°C bake
15 — off 116 hrs.
16 — off 1.5 hrs. + O_2
17 — off 42 hrs.
18 — off 15 days + O_2

J_s
$\eta(3.6)$
$\eta(2.5)$

J_s (AMPS / CM^2)

HOURS LIFE

FIGURE 10

PHOTOELECTRONS / QUANTUM at 2.5 ev x 10^6 η(2.5)

PHOTOELECTRONS / QUANTUM at 3.6 ev x 10^5 η(3.6)

FIGURE 11

TOTAL PHOTOELECTRIC YIELD FROM THIN FILM BaO ON A 0.024% MgNi BASE (PM2FFI)

#1 - 40.88 hrs. life at 800°C (.312 a/cm²)

#2 - 40.88 hrs. life at 800°C + O₂ (.007 a/cm²)

#3 - 45.95 hrs. life at 800°C (.244 a/cm²).

FIGURE 12

DECAY OF PHOTOELECTRIC YIELD AT 2.5ev
FROM THIN FILM BaO ON 0.024% MgNi
AFTER 40.88 HOURS LIFE (PM2FFI)

FIGURE 13

PULSE EMISSION, CONDUCTIVITY, AND
INTEGRATED Sr EVOLUTION VS. HOURS LIFE
FROM CATHODE SH3 - FF I

CATHODE BASE 0.024% Mg Ni
T = 1073°K, CARBONATE COATING 0.002" THICK

FIGURE 14

PULSE EMISSION, CONDUCTIVITY, AND
INTEGRATED Sr EVOLUTION VS. HOURS
LIFE FROM CATHODE SH3-FF2.

CATHODE BASE 0.024% Mg Ni.   T=1073°K
CARBONATE COATING 0.0035" THICK
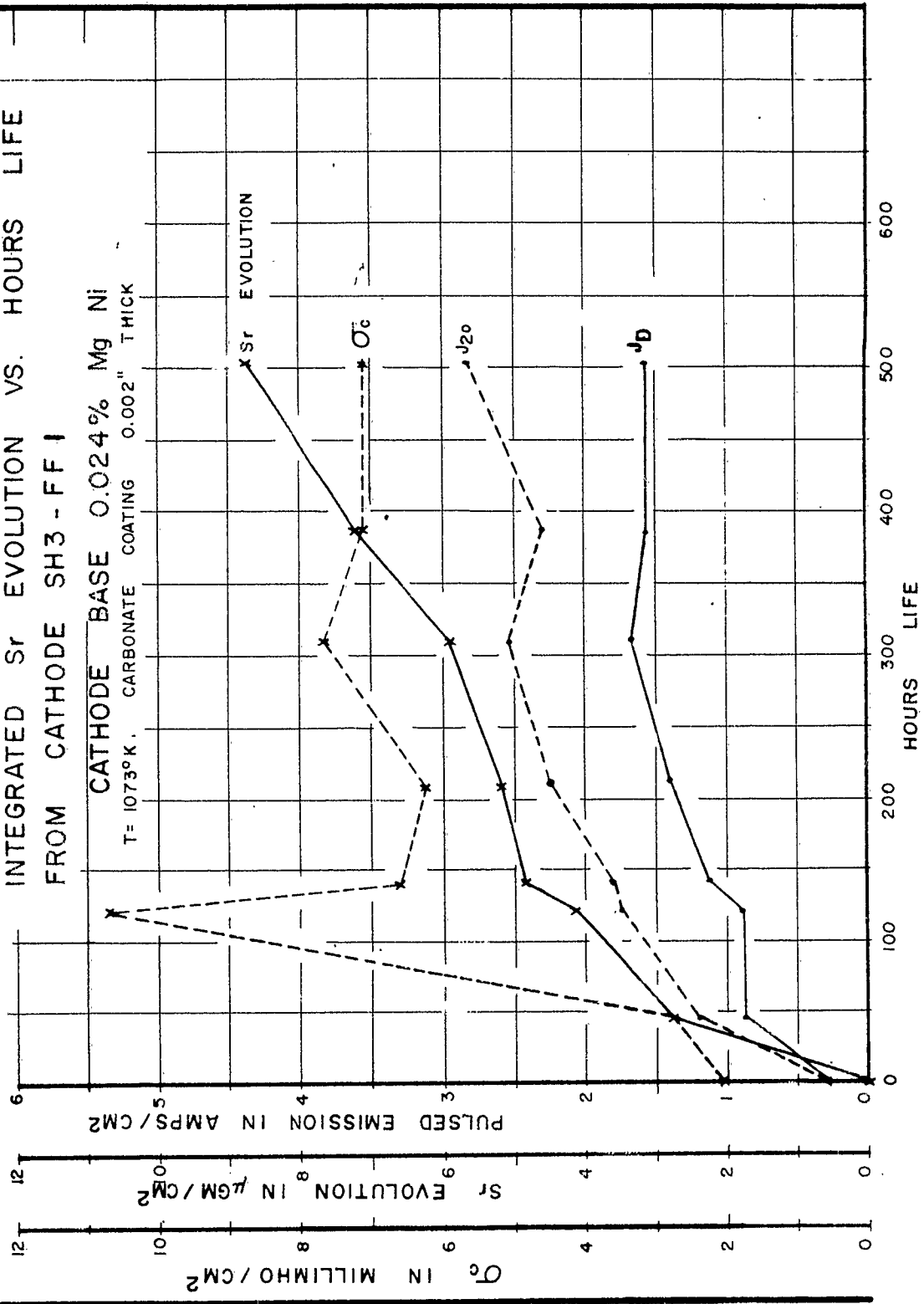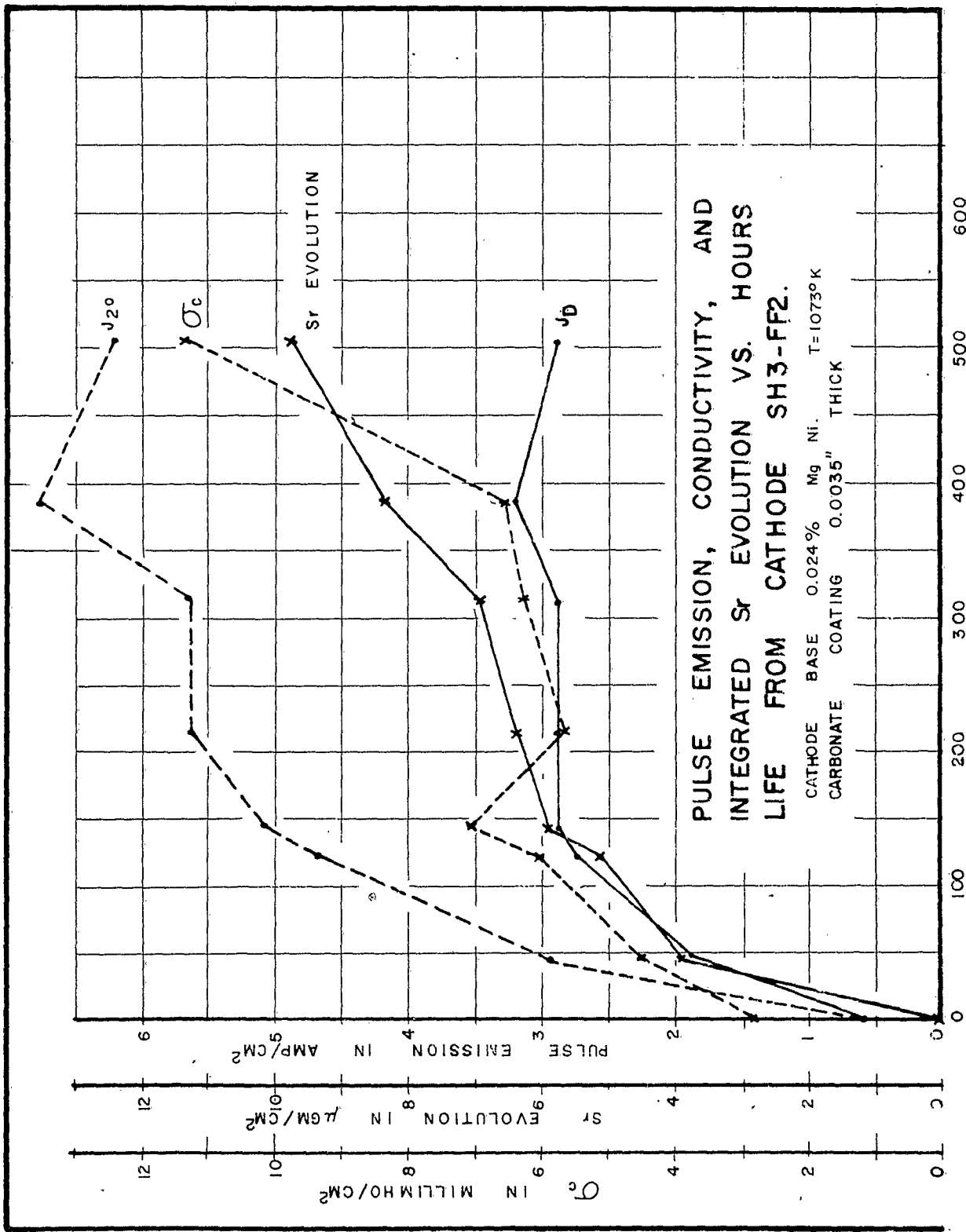
FIGURE 15

PULSE EMISSION, CONDUCTIVITY, AND INTEGRATED Sr EVOLUTION
VS HOURS LIFE FROM CATHODE SH3-FF4. CATHODE BASE
0.024 % Mg Ni. T=1073°K

CARBONATE COATING 0.0039" THICK

FIGURE 16

PULSE EMISSION, CONDUCTIVITY, AND INTEGRATED Sr EVOLUTION VS. HOURS LIFE FROM CATHODE SH4 - FF3. T=1073°K

CATHODE BASE 0.024% Mg Ni
CARBONATE COATING 0.0038" THICK

FIGURE 17

PULSE EMISSION, CONDUCTIVITY, AND INTEGRATED Sr EVOLUTION VS. HOURS LIFE FROM CATHODE SH4-FF4. CATHODE BASE 0.024% Mg Ni

CARBONATE COATING 0.0024" THICK
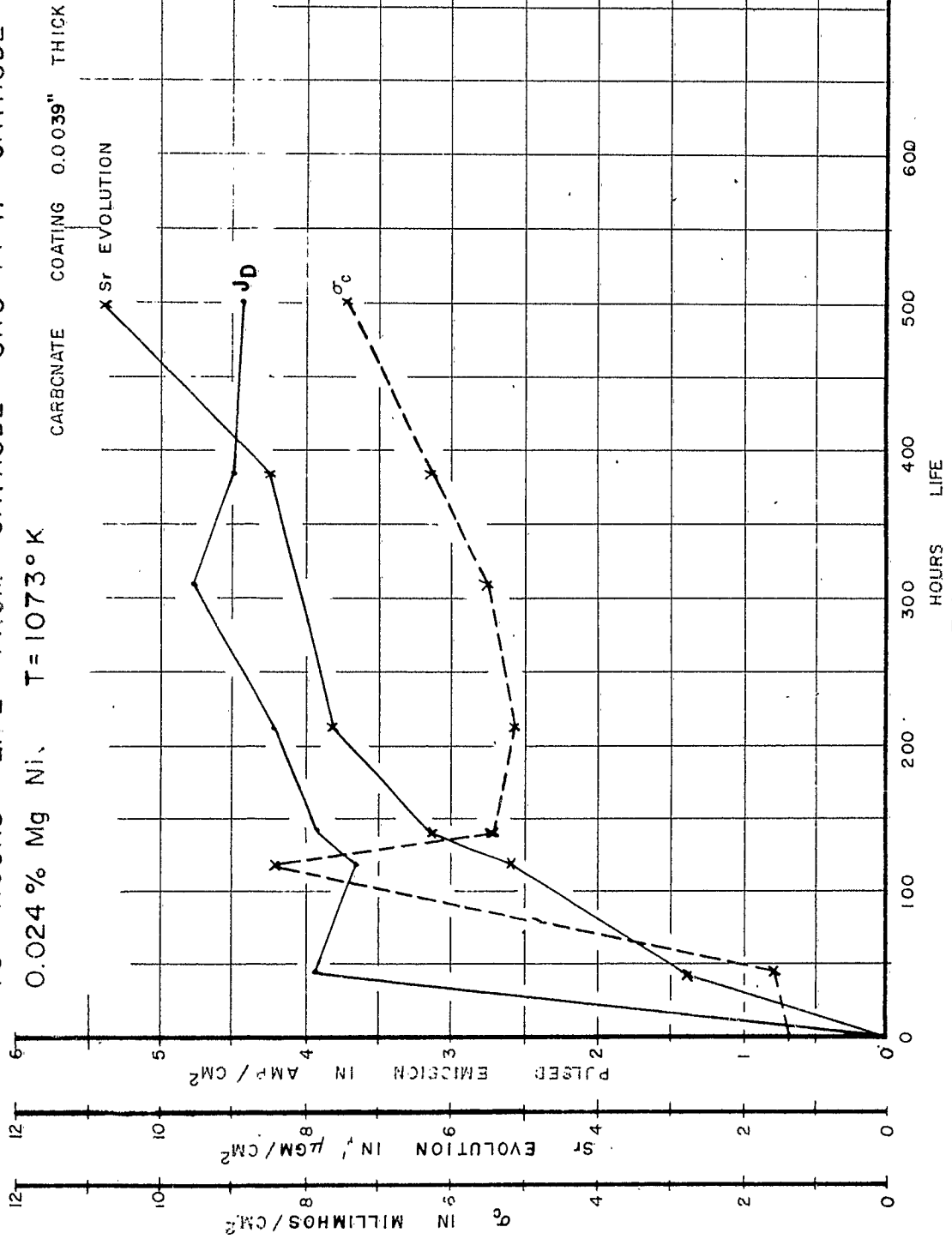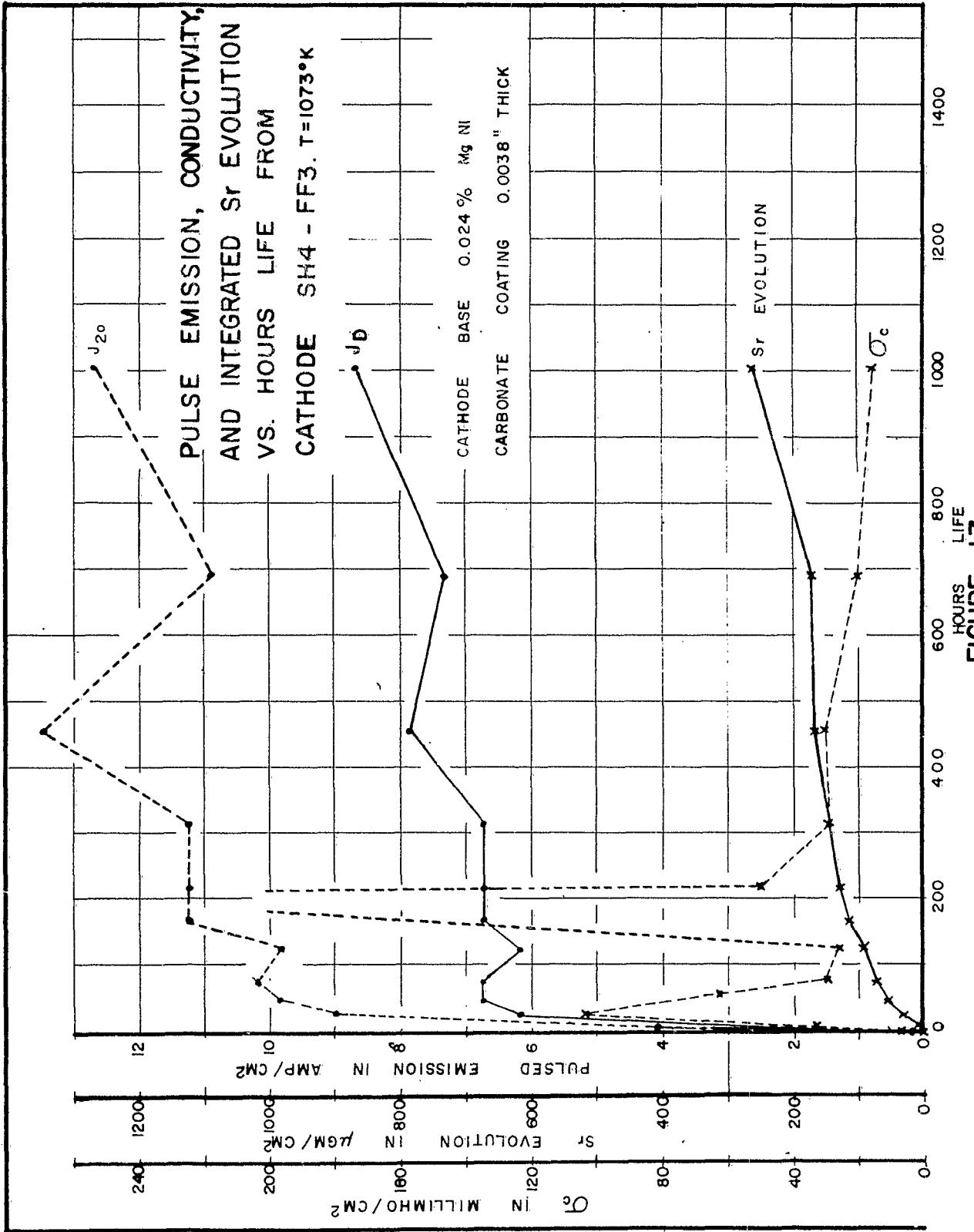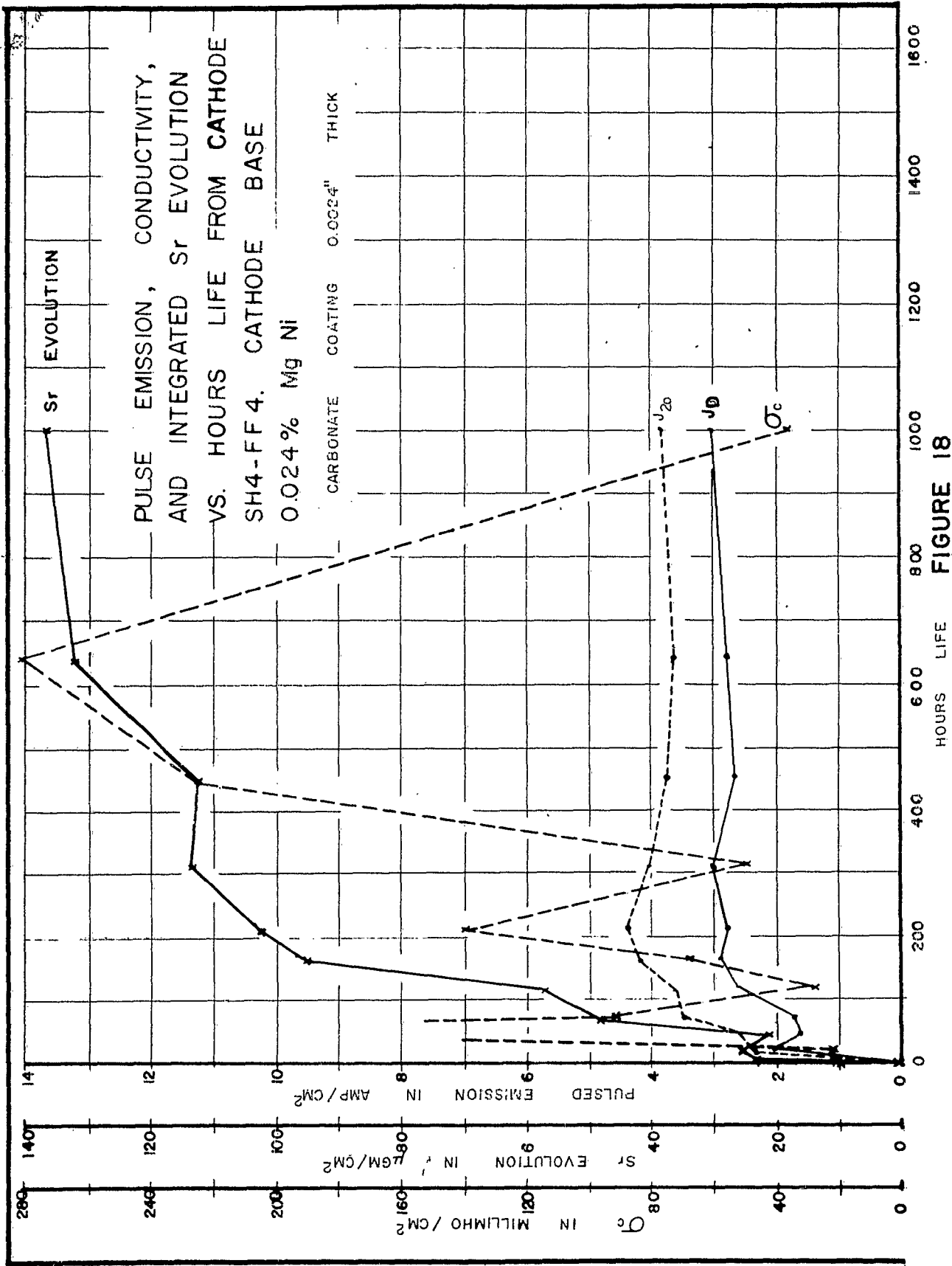
FIGURE 18

DIAGRAM OF STRUCTURE USED FOR

OXYGEN ION BOMBARDMENT

Ta ELECTRODE CONNECTED TO
FILAMENTS

$3 - \frac{1}{2}" \times .001" \times .040"$ FILAMENTS

Ta ANODE

FLATTENED GLASS

B

ENVELOPE

HINGED SHIELD

GRID

$1" \times \frac{1}{4}"$ SAMPLES
IN HOLDERS.

DUMMY SAMPLE
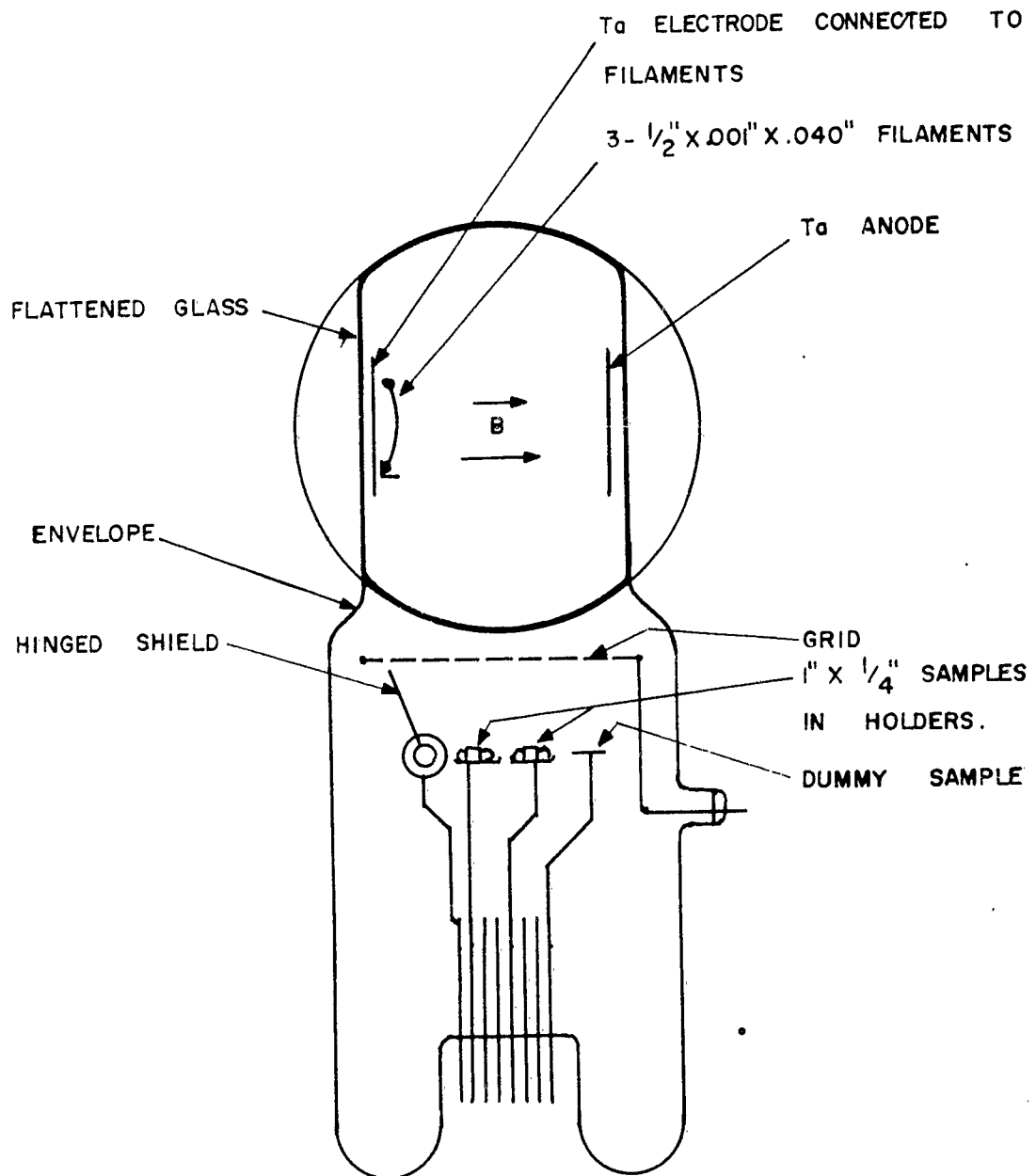
FIG. 19

BLOCK DIAGRAM OF COMPLEX IMPEDANCE
MEASURING CIRCUIT.
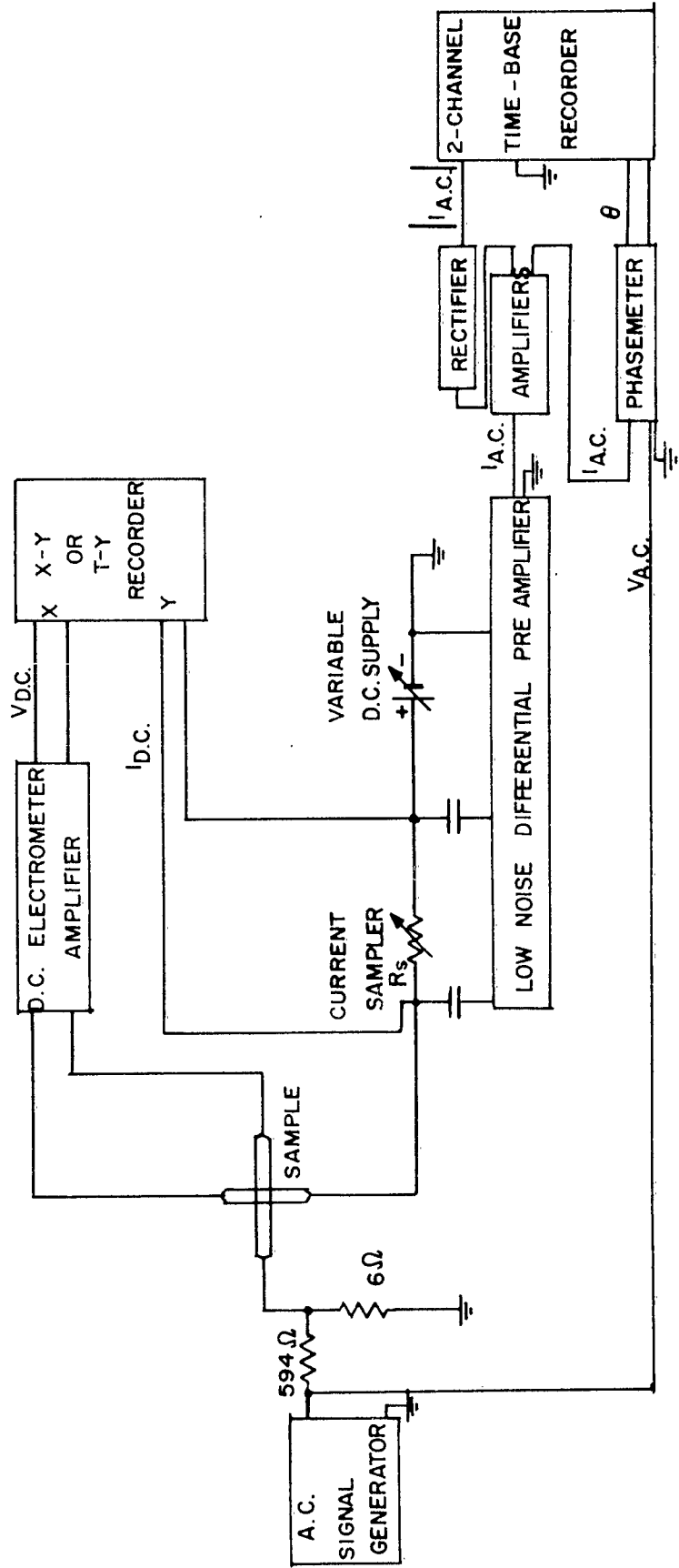
FIG. 20

I-V   CHARACTERISTICS   FROM   AI-IO,

#3   OVERLAYER   NEGATIVE.

A.C. MEASUREMENTS   OBTAINED

SIMULTANEOUSLY.
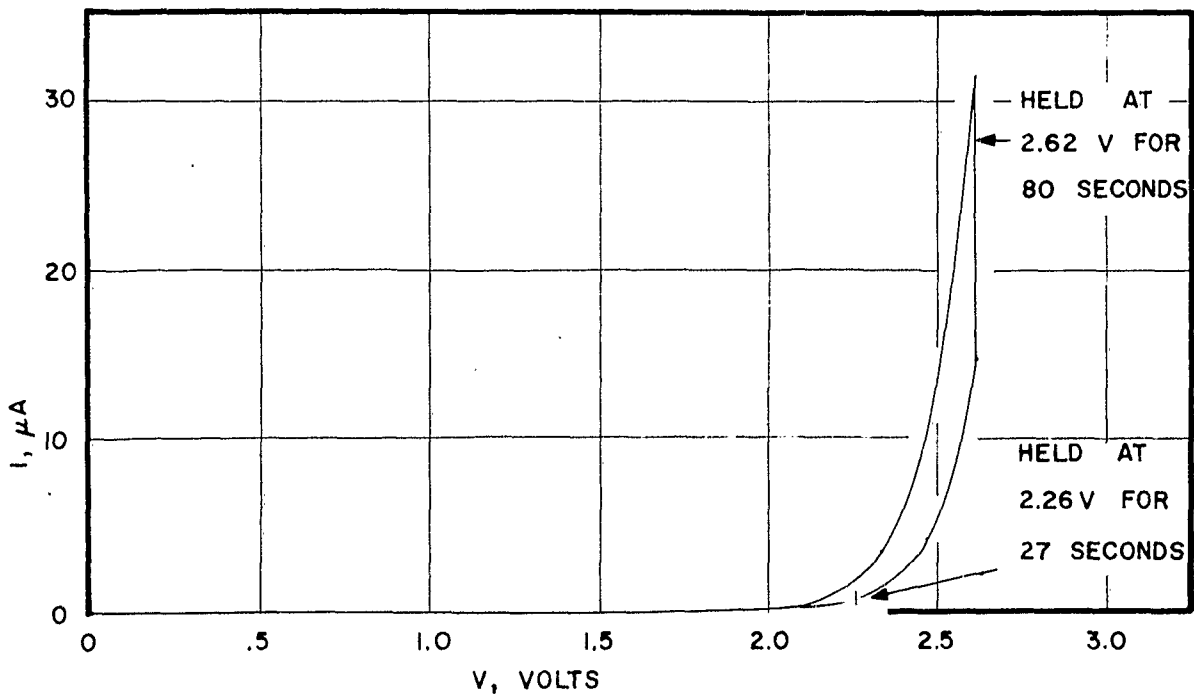
FIG. 21a
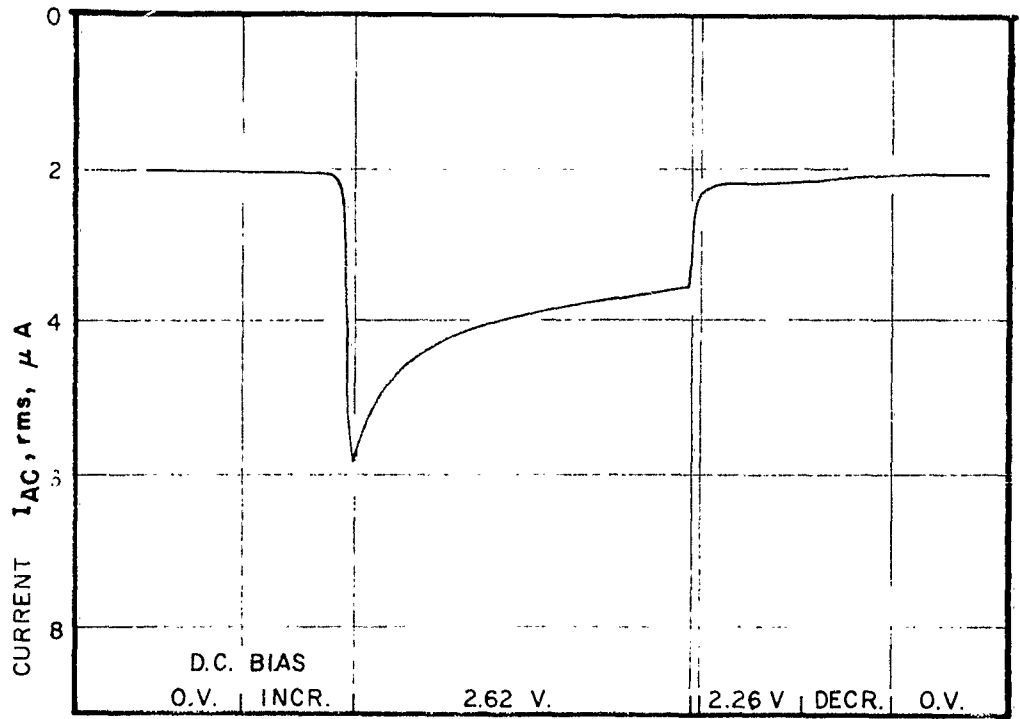
AC. CURRENT AND PHASE ANGLE VS

TIME FROM AI- IO, OVERLAYER 3, NEGATIVE

TIME, SECONDS
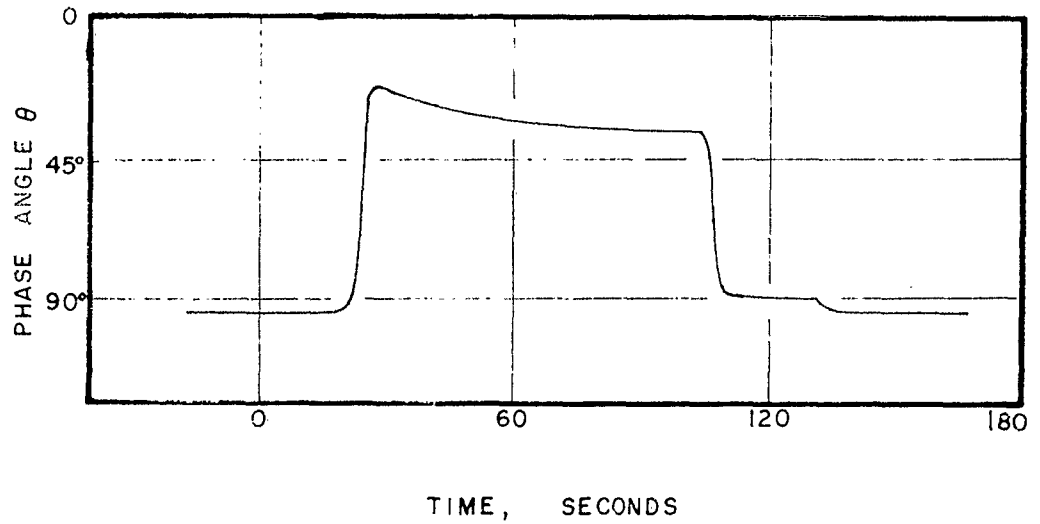
FIG. 2Ib

PARALLEL R-C EQUIVALENT VALUES
FOR AI -10, #3 OVERLAYER NEGATIVE
AS A FUNCTION OF TIME AND D.C. BIAS

FIG. 22

SUBSTRATE

W END PLATE

Ta ANODE RINGS

W FILAMENTS

TUBULATION TO ION GAUGE, ARGON SOURCE, AND Ti SPUTTER-PUMP

Au SPUTTERING TARGET

MgO SPUTTERING TARGET

B, 80-300 GAUSS
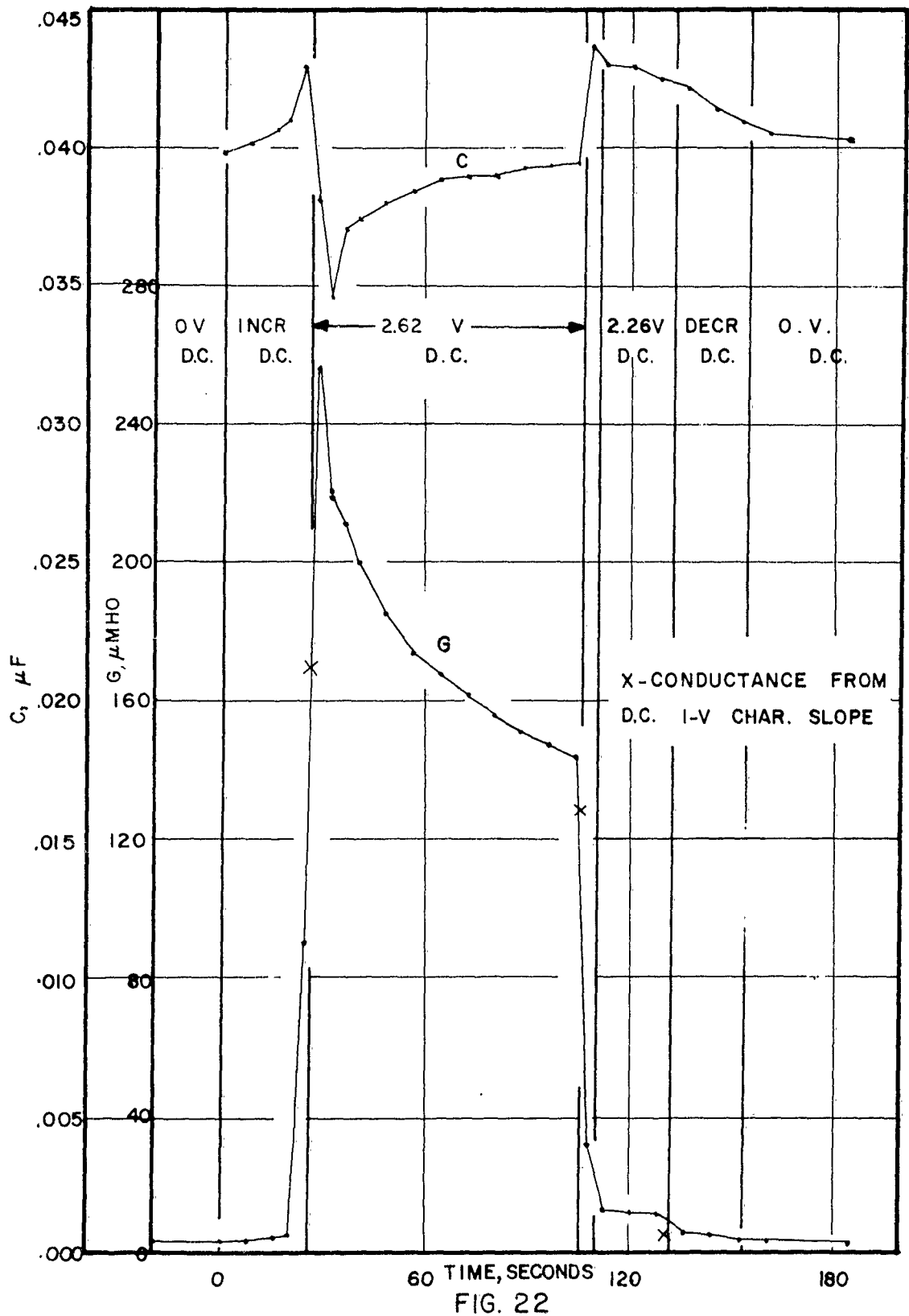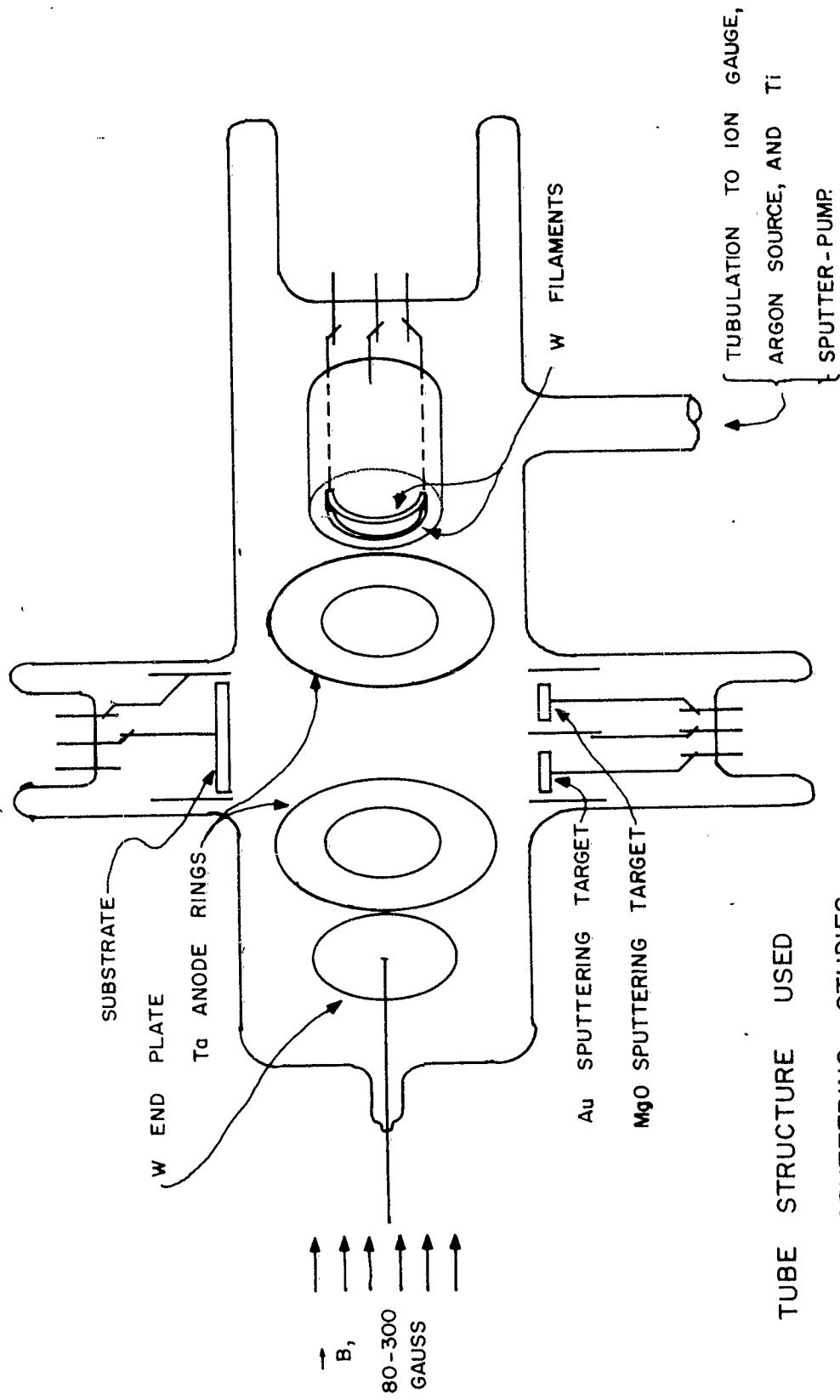
FIG. 23

TUBE STRUCTURE USED
FOR SPUTTERING STUDIES

CIRCUIT   USED   FOR

SPUTTERING   STUDIES

SUBSTRATE   ANODE   RINGS   (GROUND)

FIL.
SUPPLY
0-25 A
A.C.

MgO TARGET   AuTARGET

ANODE
SUPPLY
0-50 V D.C.

R-F
TRANS-
MITTER
3.9-6Mc
100WATT

D.C.
SPUTTERING
SUPPLY
770 V.

0.005 μf, 2KV CAPACITOR
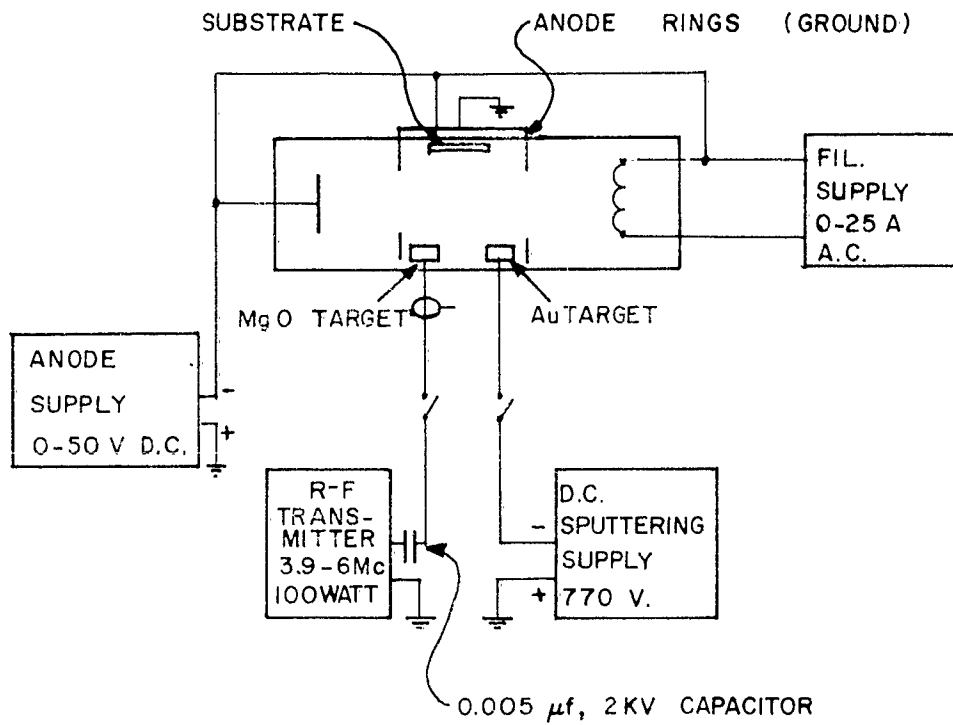
FIG. 24

I-V CHARACTERISTICS   OF

A   Ta- Ta$_2$O$_5$ - Au   SAMPLE

Ta - 44

SPUTTER   DEPOSITED   Ta

65.6 Å   OXIDE   LAYER
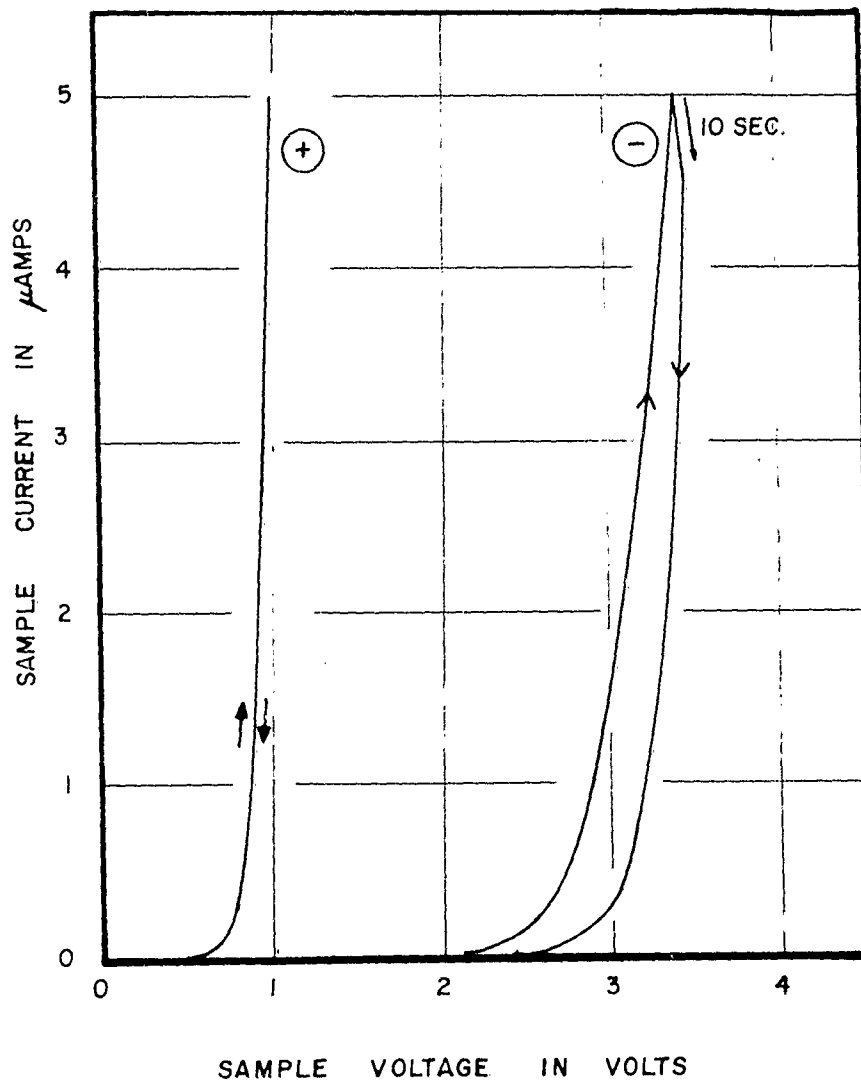
FIG. 25

FIG. 26
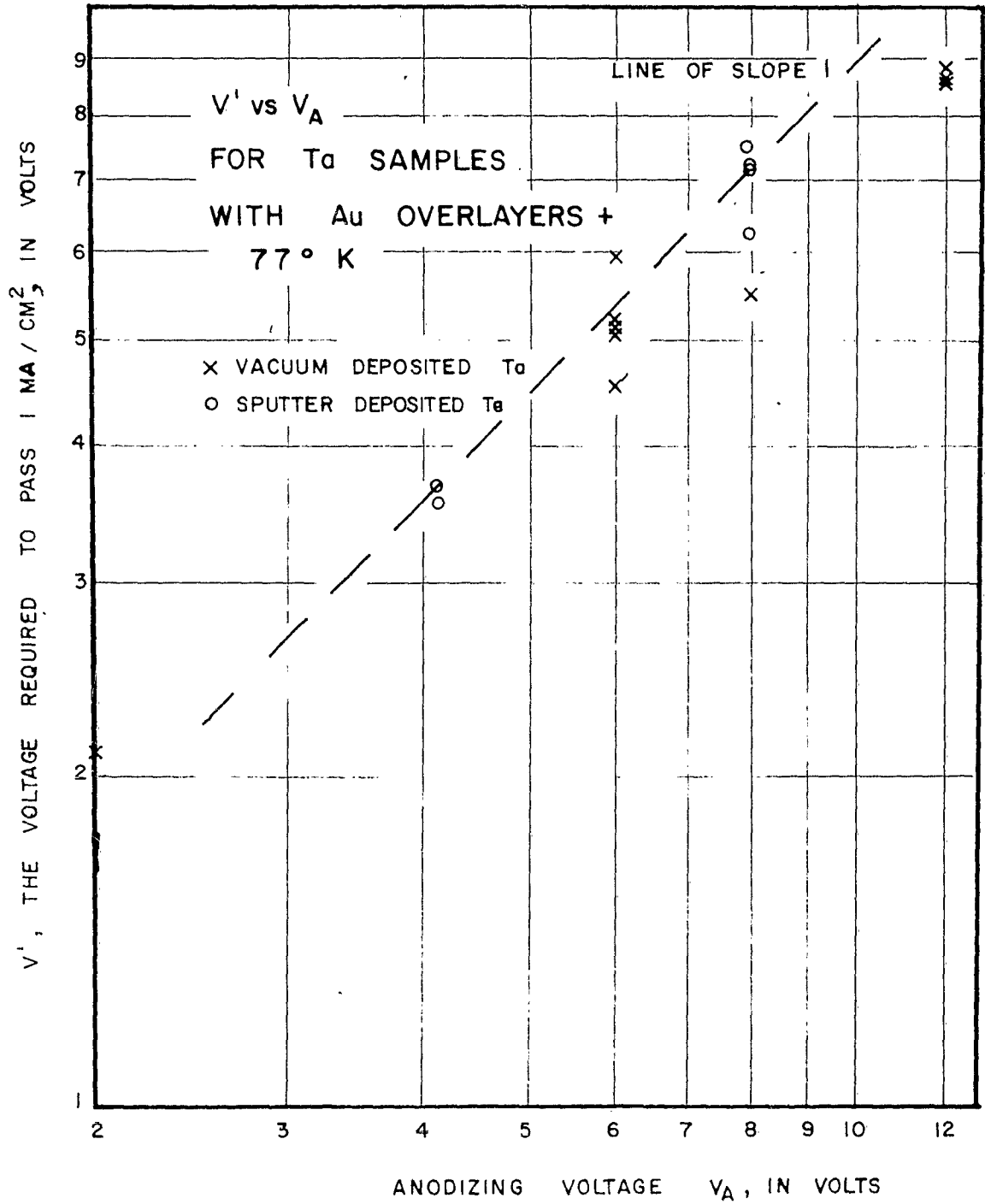
FIG. 27

FIG. 28

FIG. 29

V' vs V_A FOR Ta SAMPLES WITH Au OVERLAYERS — 77° K

X – VACUUM DEPOSITED Ta
O – SPUTTER DEPOSITED Ta

LINE OF SLOPE 1

6 POINTS

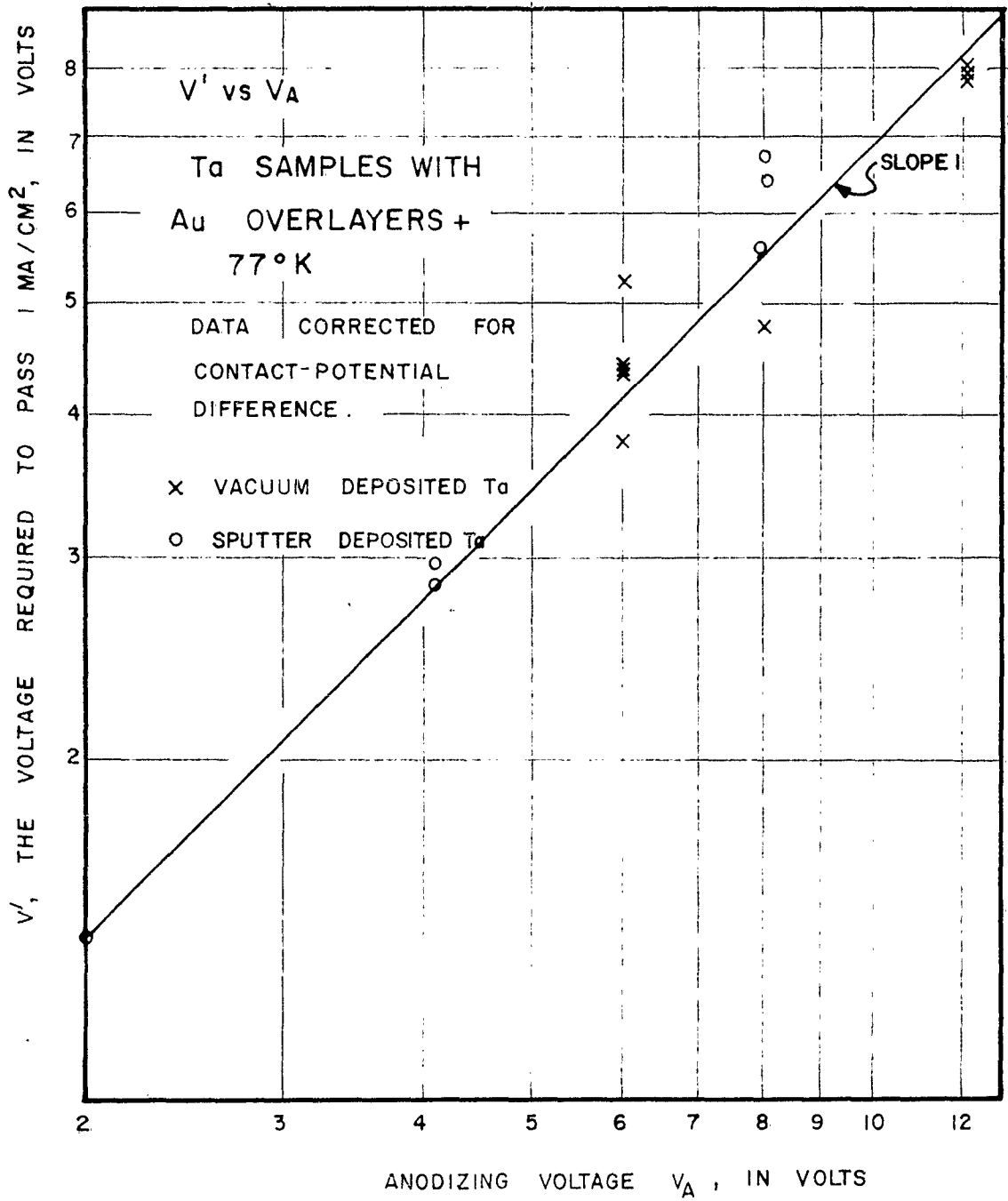V', THE VOLTAGE REQUIRED TO PASS 1MA/CM^2, IN VOLTS
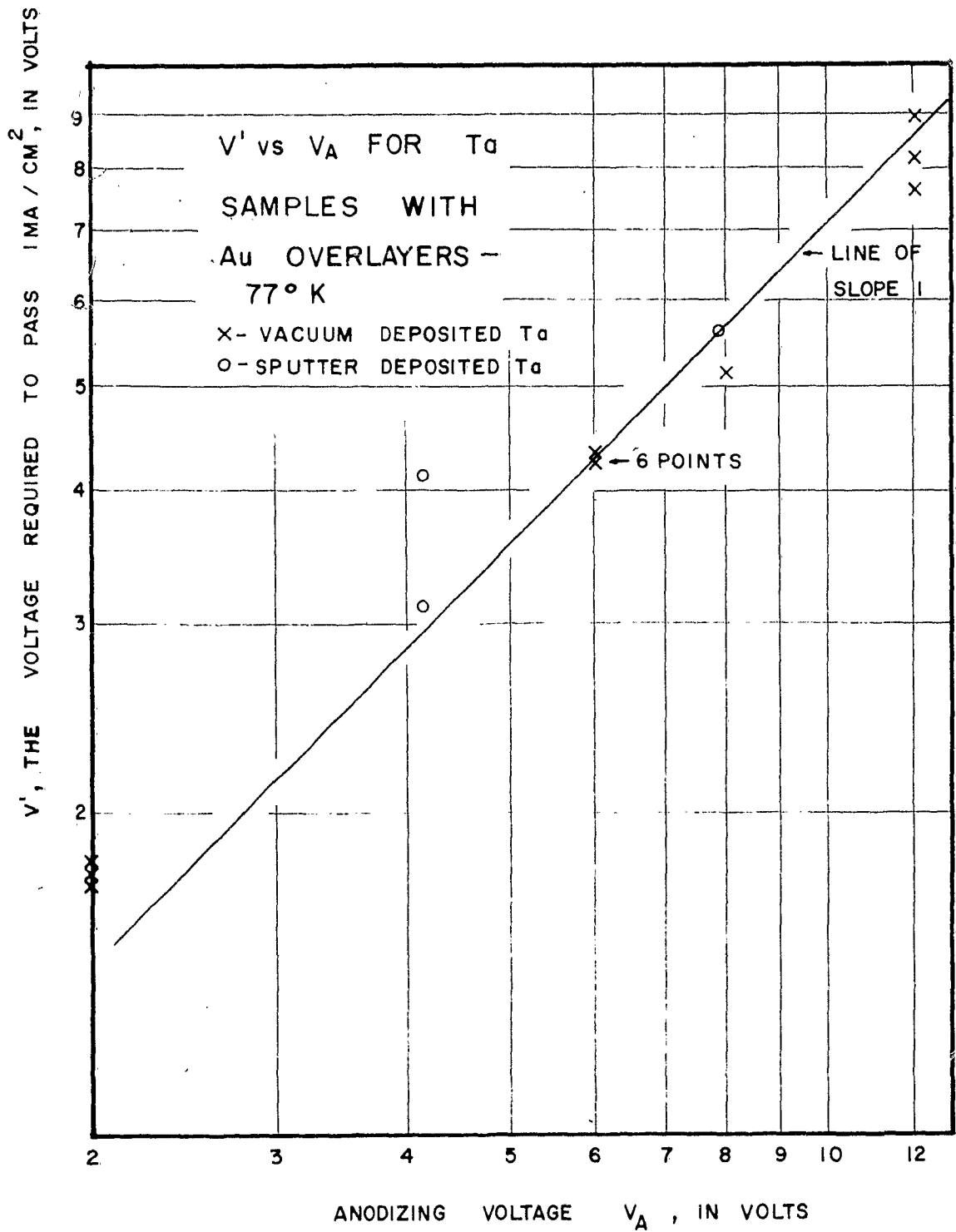
ANODIZING VOLTAGE V_A, IN VOLTS
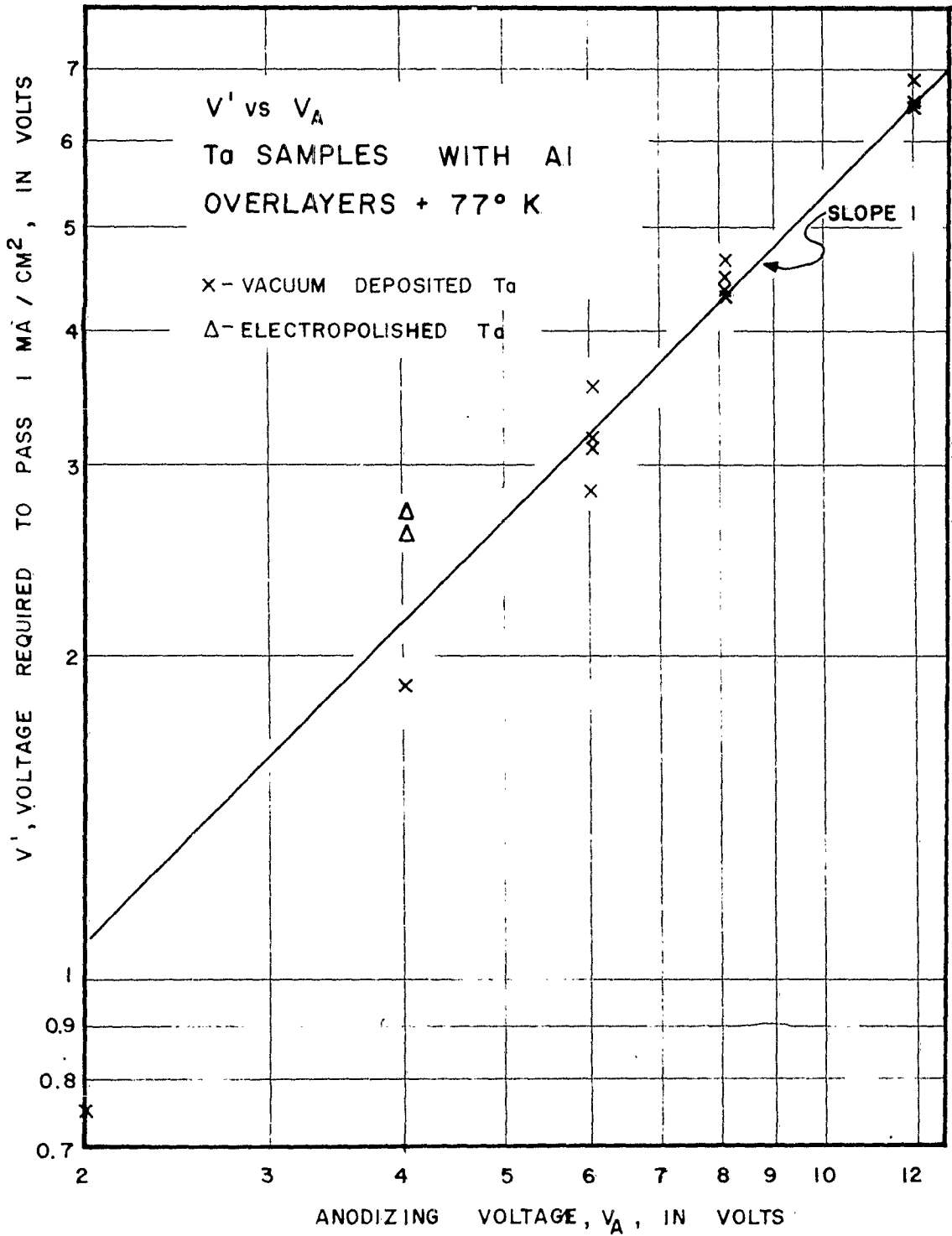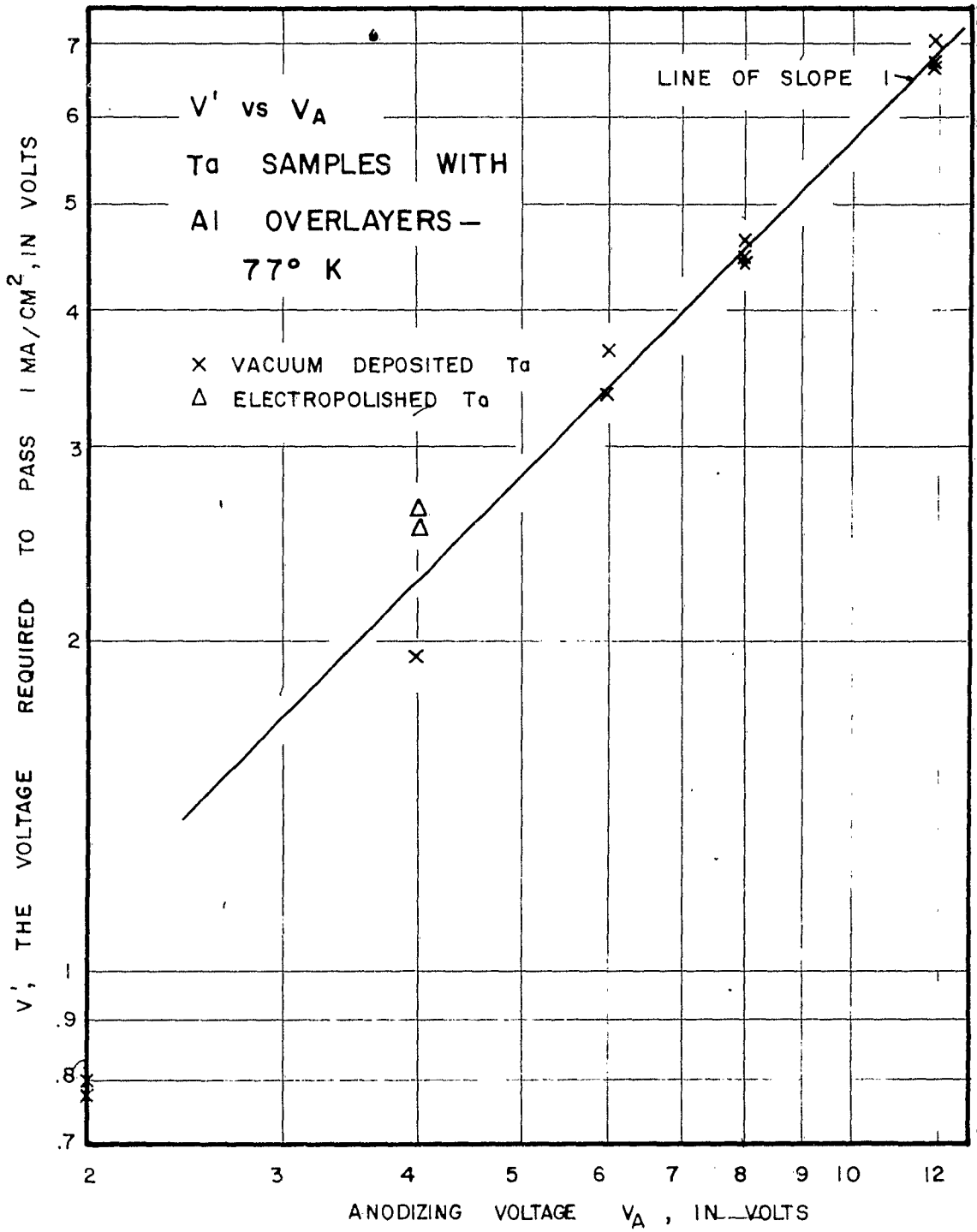
FIG. 30

Air Force Cambridge Research Laboratories, Office of Aerospace Research, Laurence G. Hanscom Field, Bedford, Massachusetts
Rpt Nr AFCRL-63-59, STUDIES OF PRIMARY ELECTRON SOURCES. Scientific Report No. 5, February 1963, 69 pp. illus., 17 refs.   Unclassified Report

A new structure for chemically reducing (BaSr)O cathodes using carbon is described. An analysis of thermal changes in cathodes under long pulse current drain, and computer solutions to the equations resulting from the analysis, are presented and the problem of cathode sparking is discussed

(over)

in terms of the indicated thermal instability. Further studies of the dependence of cathode properties of coating thickness and of photoemission from BaO are presented. Preparation of thin oxide films on vacuum-deposited Al and Be layers by reaction with an oxide atmosphere, and of MgO films by ion sputtering in an inert gas discharge, is described. The sputtering technique is also applied to produce Ta films as substrate materials. A system for monitoring the complex impedance of tunnel devices as a function of time and of dc bias is described.

Unclassified

1. Cathodes (Electron Tubes)
2. Cold Cathode Tubes
3. Field Emission
4. Oxide Cathodes
5. Superconductors
6. Thermionic Emission
7. Thin Films
I. Project 4619 Task 46190
II. Contract AF 19(604)-8381
III. Electron Tube Research Laboratory, University of Minnesota,

Institute of Technology
IV. Prepared by D. E. Anderson